energies

MDPI

Review

A Comprehensive Review of Strategies and Approaches for Enhancing the Performance of Thermoelectric Module

Song Lv [1,2,*], Zuoqin Qian [1], Dengyun Hu [2], Xiaoyuan Li [3] and Wei He [4]

[1] School of Energy and Power Engineering, Wuhan University of Technology, Wuhan 430070, China; chwhqzq@163.com
[2] Department of Thermal Science and Energy Engineering, University of Science and Technology of China, Hefei 230026, China; dengyunhu@mail.ustc.edu.cn
[3] School of Information Engineer, Wuhan University of Engineering Science, Wuhan 430200, China; lixiaoyuan198306@163.com
[4] Department of Building Environment and Equipment, Hefei University of Technology, Hefei 230009, China; jimminyhe@126.com
* Correspondence: lvsong@mail.ustc.edu.cn

Received: 9 May 2020; Accepted: 2 June 2020; Published: 17 June 2020



Abstract: In recent years, thermoelectric (TE) technology has been emerging as a promising alternative and environmentally friendly technology for power generators or cooling devices due to the increasingly serious energy shortage and environmental pollution problems. However, although TE technology has been found for a long time and applied in many professional fields, its low energy conversion efficiency and high cost also hinder its wide application. Thus, it is still urgent to improve the thermoelectric modules. This work comprehensively reviews the status of strategies and approaches for enhancing the performance of thermoelectrics, including material development, structure and geometry improvement, the optimization of a thermal management system, and the thermal structure design. In particular, the influence of contact thermal resistance and the improved optimization methods are discussed. This work covers many fields related to the enhancement of thermoelectrics. It is found that the main challenge of TE technology remains the improvement of materials' properties, the decrease in costs and commercialization. Therefore, a lot of research needs to be carried out to overcome this challenge and further improve the performance of TE modules. Finally, the future research direction of TE technology is discussed. These discussions provide some practical guidance for the improvement of thermoelectric performance and the promotion of thermoelectric applications.

Keywords: thermoelectric conversion; TE module; thermoelectric cooler; energy efficiency; performance improvement approaches

1. Introduction

With the rapid development of the economy and the improvement of people's quality of life, the energy crisis and environmental problems are becoming increasingly serious, which has gradually attracted the attention of all countries in the world. Therefore, the development of renewable energy has become a hot topic. However, there are still many difficulties in their utilization. Therefore, the development of sustainable technologies to effectively use, convert and recycle waste energy is another way to solve the problem. Being no moving parts, environment friendly, requiring almost no maintenance, and directly converting heat into electricity, thermoelectrics has become one of the most promising methods to solve environmental pollution and energy problems. Thermoelectrics has many

practical applications that range from renewable energy utilization to the utilization of industrial waste heat [1]. Moreover, thermoelectrics not only generate electric energy from heat, but can also be used as a heat pump based on the Peltier effect. To date, the application of thermoelectric technology has been extended to aerospace, vehicles, industrial equipment, energy-saving buildings, medical devices and electronic devices. Thermoelectric technology is a research hotspot in this period, which has attracted many researchers' interest. Thermoelectric technology is usually applied in the form of thermoelectric modules. However, although the module has been out for a long time, its low efficiency and high cost hinder its wide application and commercialization. Existing thermoelectric converters could not compete with existing alternatives such as organic Rankine cycles or compression refrigeration. As a result, immense efforts have been made to improve the energy-conversion efficiency and enhance the thermoelectric performance of thermoelectric (TE) devices. The continuous efforts to improve thermoelectric conversion based on the working principles of TE can be divided into three categories: (1) the improvement of the material; (2) the optimization of the structure/geometry of the thermocouple or TE module; and (3) the improvement of the thermal management.

There are many reviews of thermoelectricity, mainly for materials [2], devices [3], and its application [4]. This work is therefore aimed at accommodating better insights and carrying out a comprehensive review of the strategies and progresses of improving the thermoelectric conversion efficiency and their performance. A brief background and the basic principles of thermoelectrics is covered first, which provides a theoretical basis for the enhancement of thermoelectric performance. Section 3 deals with the improvement of the thermoelectric module while Section 4 discusses the optimization of the thermal management system of TE systems. The influence contact resistance and their improvement methods are presented in Section 5. At the end of the paper, the technical obstacles of improving the efficiency of thermoelectrics are summarized, and the future research work is prospected. It provides different insights and further guidelines of how to improve the thermoelectric conversion efficiency of thermoelectric devices.

2. Basic Principle of Thermoelectrics

Thomas Johann Seebeck observed in 1821 that when two different metals were brought together and there were different temperatures at the connection, a current electromotive force was generated in the connection circuit which was proved by the change of the magnetic field. In addition, in 1834 J.C.A.Peltier discovered that two joint dissimilar metals do not only generate electricity from heat, but the opposite can also happen. When there is an electric current, the joints of different conductors absorb or reject the heat according to the direction of the current. Based on the discovery of this phenomenon, eventually a thermoelectric effect and the thermoelectric materials are developed [5]. The typical TE module consists of a bunch of thermocouples made of n-type and p-type materials wired together. A pair of thermocouples in a TE module working as an electric generator and a heat pump is schematically shown in Figure 1.

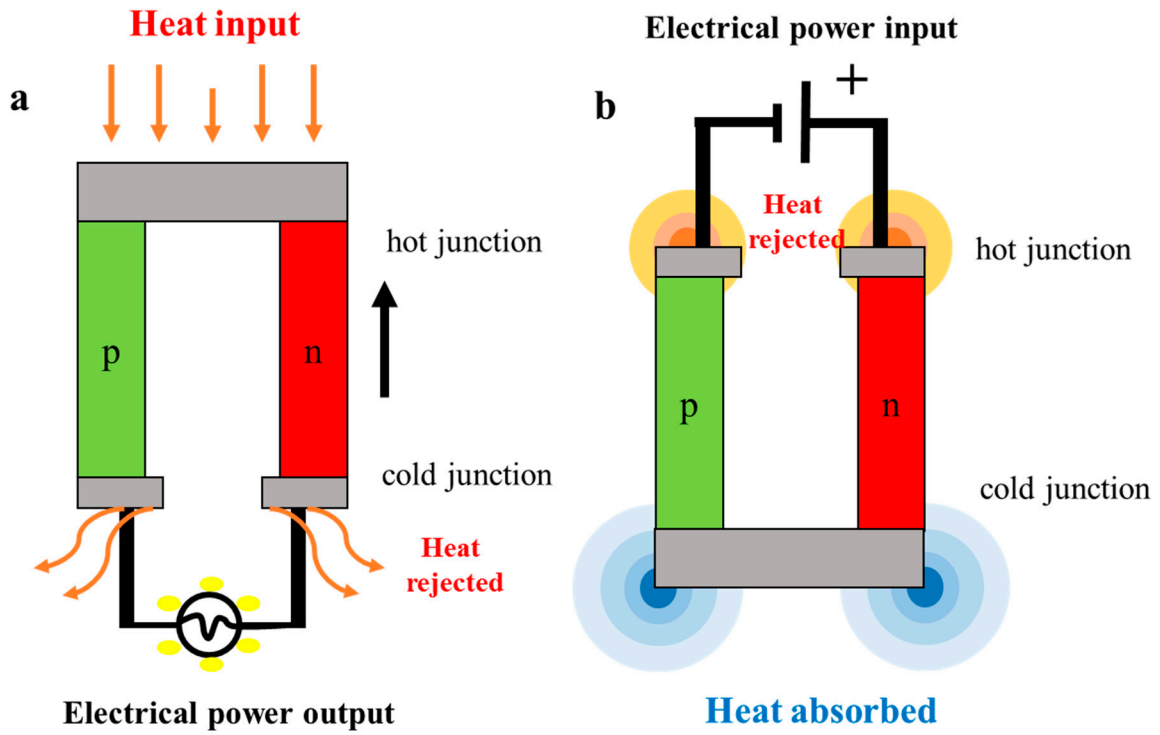


Figure 1. Representation of the Peltier (**a**) and the Seebeck (**b**) effect. Reproduced from [6].

In the TE element, the charge carriers are transmitted by p–n junctions, and electrons/holes act as "fluids". The applied temperature gradient produces the carrier gradient and then generates electrostatic potential. In thermoelectric cooling, the reverse process occurs: the current produces a heat flow at the junction of p-type and n-type materials.

The figure of merit (Z) is a commonly used parameter used to evaluate thermoelectric material:

$$Z = \frac{\alpha_{p,n}^2 \sigma_{p,n}}{\lambda_{p,n}} \tag{1}$$

where $\alpha_{p,n}$ stands for the Seebeck coefficient, $\sigma_{p,n}$ is the electrical conductivity, and $\lambda_{p,n}$ is the thermal conductivity.

In addition, a dimensionless parameter, the figure of merit (ZT), could be written as:

$$ZT = \frac{\alpha^2 \sigma T}{\lambda} \tag{2}$$

where T is the operating temperature. These four parameters α, σ, λ and T depend on each other. It can be learned from formula (2) that a good TE material should have a good conductivity and poor thermal conductivity, as well as a high Seebeck coefficient. In theory, ZT has no basic maximum limit. In addition, based on the use of known material optimum values, it is possible that the ZT value is greater than 4 [7]. The ZT value of thermoelectric material should be bigger than three for commercialization [8].

Moreover, the conversion efficiency of the thermoelectric module acting as an electrical generator or heat pump could be written as:

$$\eta = \frac{T_h - T_c}{T_h} \cdot \frac{\sqrt{1+ZT}-1}{\sqrt{1+ZT}+T_c/T_h} \tag{3}$$

$$COP = \frac{T_c}{T_h - T_c} \cdot \frac{\sqrt{1+ZT}-T_h/T_c}{\sqrt{1+ZT}+1} \tag{4}$$

where η is the thermoelectric conversion efficiency, T_h and T_c are the temperatures of the cold and hot sides of the TE module, respectively.

The figure of merit (ZT) and Equations (3) and (4) demonstrate that the improvement of a thermoelectric module could be obtained by improving the Seebeck coefficient, reducing the thermal conductivity and managing the temperature. To go along with this, nowadays, there are three main action strategies to improve the conversation coefficient of η (main for power generation) or COP (main for refrigeration). The first strategy is directed at enhancing the performance of thermoelectric materials by increasing the ZT with certain approaches/strategies. The second strategy aims to improve thermoelectric modules by optimizing the structure/geometry of thermocouples or modules, or by using scalable manufacturing techniques. The third line of strategy in order to enhance the performance of thermoelectric modules is focused on thermal system management to optimize the temperature difference between the two sides of the TE modules. Therefore, this review is focused on these three aspects. The details are discussed in the following sections.

3. Development of High-Efficiency Thermoelectric Modules

Over the years, a great deal of efforts has been made to improve thermoelectric performance, and we have witnessed the rapid development of thermoelectric research. Some new concepts and examples are described here, which aim at superior TE materials and higher TE performance. Generally, recent studies have focused on novel nanostructured thermoelectric materials. In addition, the properties of classical materials have been significantly improved, including the improvement of classic TE material properties (such as doping, alloying, inserting foreign species and nanostructure), organic TE materials [9], and increasing the ZT values of thermoelectric materials by nanotechnology [10], the optimization of the structure/geometry of thermocouples or developing the novel thermoelectric module shapes [11]).

In recent years, with the development of nanostructure engineering, people are more and more interested in thermoelectric devices, which makes people devote themselves to display efficient nanostructured materials such as the alloyed nano-system, superlattices, nanowires and quantum dots. Table 1 lists some thermoelectric materials obtained in recent years by different improving methods and their thermoelectric properties.

Table 1. Some different thermoelectric materials and their thermoelectric properties.

Application	Material	ZT	Temperature, K	Ref
Power generations	$Cu_xSn_1S_4$	0.6	370~570 K	[12]
	Phase-separated $PbTe_{0.7}S_{0.3}$	>2	673~923 K	[13]
	$Mm_{0.9}Fe_{3.5}Co_{0.5}Sb_{12}$-based	0.9	773~973 K	[14]
	Bi_2Te_3/Sb_2Te_3 superlattice	2.4	Room temperature	[15]
	$Bi_2(Te,Se)_3$ nanowire array	1.01	Room temperature	[16]
	$PbTe_{(1-x)}Se_{(x)}$ alloys	1.5	400~900 K	[17]
	3,4-Ethylenedioxythiophene	0.42	Room temperature	[18]
Heat engine	CdZnTe		283 K~313 K	[19]
	Sb_2Te_3/Bi_2Te_3 $Bi_2Te_{3-x}Se_x$	1.5	Room temperature	[20]
	Bi2Te3-based thin-film superlattice	>2		[21]

In this section, we mainly discuss some methods that can significantly improve the performance of materials such as doping/alloying, superlattices, other nanostructures, and structure/geometry.

3.1. Thermoelectric Material

The material used in the TE module has an important influence on its performance. Many researchers have done a lot of work to improve the performance of TE material, and some significant advances have been made in improving its properties in recent years. The performances of lots of thermoelectric materials

have been improved and new materials have been developed. These materials range from semiconductors to ceramics [22,23], from bulk to superlattice [24,25] and from nanoparticles to nanowires [16–27].

3.1.1. Doping/Alloying

The key to design high-performance thermoelectric materials is to improve the strong correlation of *S*, σ and *K* by carrier concentration n. In the ideal case, the Seebeck coefficient is directly decided by the bandgap, the carrier concentration and the charge carriers' mass. Moreover, it will vary linearly with the absolute temperature. Thus, it is found that carrier concentration n is the key to adjust the peak temperature and the maximum power factor ($S^2\sigma$).

The relationship between the carrier concentration and the Seebeck coefficient could be written as

$$S = \frac{8\pi^2\kappa_B^2}{3eh^2} m^* T \left(\frac{\pi}{3n}\right)^{2/3} \quad (5)$$

where m^* is the effective mass of the charge carrier, h is Planck's constant, κ_B is the Boltzmann constant, and e is the carrier charge.

For inorganic semiconductors, proper doping can improve the carrier concentration in thermoelectric material by changing their electronic band structure. Therefore, as the appropriate dopant atoms continue to grow, the number of states in each level will also increase. The energy states close to the Fermi level can promote electron transport. For organic materials, according to band theory, the highest occupied energy levels of atoms in the lattice form the valence band, and the lowest vacancy electronic levels form the conduction band; when the band gap between the two bands is small enough to make the electrons move from the valence band to the conduction band under excitation, the conductivity in the semiconductor is produced. Thus, by introducing defects, doping can introduce an additional energy level between the two bands, thereby increasing conductivity [26].

Figure 2 shows the Seebeck coefficient and conductivity varying with the change of the carrier concentration. Obviously, the charge-carrier concentration has a great effect on them, and with the increase in carrier concentration, the conductivity increases but the Seebeck coefficient decreases.

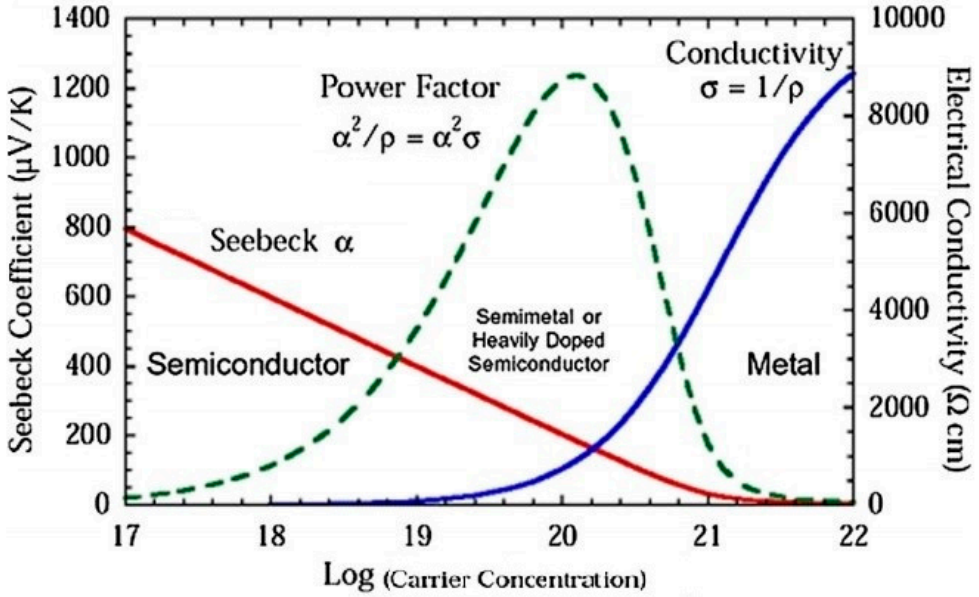


Figure 2. The electrical properties of the thermoelectric materials vary with the carrier concentration. Reproduced from [27].

Thus, to improve σ, doping is an effective way to improve the thermoelectric performance. Therefore, a virtually universally used and one of the technologically simplest and straightforward

method to improve the thermoelectric properties of TE materials is doping/alloying or inserting foreign species.

Chemical doping is widely used to tune the carrier concentration and improve the figure of merit ZT [28–30]. SnSe, Sn, Ag and Cu [31,32] usually act as p-type dopants, while $BiCl_3$ and I [33] are n-type ones. Tremendous progress has been made in the past 20 years in the exploration of high-performance thermoelectric materials [34–36] and records of high ZT values are constantly being broken in the laboratory, such as Bi_2Te_3-based compounds [37–39], lead chalcogenides [40] and hole-doped crystals [41]. Moreover, by doping [42], alloying [43,44] and microstructure modulation [45,46], the relatively high ZT values ~1.1 of polycrystalline samples is obtained at 773–823 K. Wei et al. [47] studied the enhancement of thermoelectric properties by doping Li, K, and Na to polycrystalline SnSe. They found that all these dopants improved the carrier concentration and conductivity of SnSe. At 800 K, the maximum ZT of ~0.8 in contrast to pristine SnSe samples, the performance was improved by 30%. Peng et al. [48] gained excellent thermoelectric properties of SnSe single crystals by doping 3% Na. Especially in the case of $Sn_{0.97}Na_{0.03}Se$, the ZT value was more than 2 at 800 K. Tan et al. [49] obtained p-type SnTe with substantially improved thermoelectric properties through In/Cd cooping. In addition, the ZT value reached 1.4 at 923 K. Lei Yang et al. [50] proposed excellent n-type PbTe-based thermoelectric materials by selecting Bi to dope PbTe nanocubes and gain a maximum ZT of 1.35 at 675 K for n-type $Pb_{0.99}Bi_{0.01}Te$. H. J. Wu et al. [13] introduced K into the phase-separation $PbTe_{0.7}S_{0.3}$ system. It not only had the peak ZT value at 923 K of 2.2, but also created the first example of the widest platform material with ZT > 2. The average ZT of 2.5% K-doped $PbTe_{0.7}S_{0.3}$ is 1.56. Zhao et al. [41] realized the hole-doped tin selenide (SnSe) crystals and obtained a maximum ZT_{dev} of 1.34, whereas Mori et al. [51] achieved a maximum ZT of 2.0 at 600 K in the $Ge_{0.92}Cr_{0.03}Bi_{0.05}Te$ by reducing the formation energy of Ge vacancies by replacing Ge with Cr. Li and G. Jeffrey et al. [52] reduced the lattice thermal conductivity (kappa(l)) by microstructure engineering and enhanced the thermoelectric figure of merit (zT).

3.1.2. Superlattices

From Equation (2), it can also be observed that reducing thermal conductivity can improve the material properties. According to the above description, the doping and alloying could also increase the Seebeck coefficient by magnifying the electron density of the states. However, the key to achieve a high ZT value is to increase the conductivity without increasing the thermal conductivity. In semiconductors, 90 % of thermal conductivity usually comes from the lattice thermal conductivity. Therefore, reducing lattice thermal conductivity will result in a significant improvement in the TE performance [53]. The thermal conductivity of materials is strongly affected by phonons produced by lattice vibrations [54]. The lattice thermal conductivity depends on the crystal structure and lattice parameters. Meanwhile, the disadvantage of heavy doping is that the superlattices can solved the Seebeck coefficient corresponding to the minimum conductivity, resulting in optimal transport/thermoelectric properties [55].

Super-lative is the periodic layers of two or more substances having a thickness of about one nanometer. Wherein the alternating layers of different materials can prevent phonon transmission through scattering by internal interface scattering and the electronic properties can remain substantially ineffective as long as the periodicity of the superlattice is properly set so that the value of the thermal conductivity in superlattices is greatly reduced has led to many theoretical studies in this field. The study of Chen Gang et al. [56] show that the thermal conductivity of nanostructures is lower than that of bulk materials. The influence of superlattice structure on lattice thermal conductivity was affected by: including the correction of phonon spectrum, the localization of the phonons, the diffuse or specular scattering of the phonons at interfaces and the scattering of phonons at defects [57]. These mechanisms have been explored through several superlattices where the composition of the material starts with fairly good TE properties, such as PbTe/PbSe [58,59], Bi_2Te_3/Sb_3Te_3 [15,58], Si/Ge [60,61] and Bi/Sb [62],

inorganic/organic [63]. As can be seen from these examples, the use of superlattice structures reduces thermal conductivity, resulting in increased ZT values.

Venkatasubramanian et al. [64] proposed for the first time the idea of using superlattices to improve the ZT value by reducing the phonon thermal conductivity. Later generations continue to explore this mechanism. They obtained a p-type Bi_2Te_3/Sb_2Te_3 superlattice device by controlling the transmission of phonons and electrons in superlattices. and the ZT of it could reach a record of 2.4 [15]. Several experimental studies have been reported in [65], which proved that the thermal conductivity of various superlattices is significantly reduced. This phenomenon leads to a large improvement in the ZT value of superlattice thermoelectrics. Harman et al. [59,62,66] manufactured a superlattice structure with $PbTe/PeSe_{0.98}Te_{0.02}$ on top of the BaF_2 substrate, and the structure achieved ZT ~1.6 and ZT ~3.5 at 300 K and 570 K, respectively. Lee et al. [67] presented thermoelectric properties of p-type $Bi_2Te_3/Bi_{0.5}Sb_{1.5}Te_3$ superlattice films. These achieved an impressively high ZT of 1.44 at 400 K, 43% higher than the original. Priyadarshi Pankaj et al. [68] analyzed various superlattice designs and concluded that a superlattice with a Gaussian distribution of barrier thickness provides maximum ZT. The high ZT value of 6 can be obtained in these cases, where the lattice thermal conductivity has been found to be much lower than the alloy limit and sometimes close to the values of amorphous phases. The main disadvantage of using superlattices is that the synthesis route is complex, the cost is high and the large temperature difference on the material cannot be supported. Niemela et al. [55] and Zhao et al. [69] made a comprehensive summary of studies on superlattices.

3.1.3. Nanostructures

As mentioned in the previous section, superlattice is a two-dimensional thermoelectric nano material. When the grain size is reduced to nano scale, the performance of thermoelectric materials can be improved, phonon scattering can be increased, lattice thermal conductivity can be reduced, and good electrical performance can be maintained at the same time [70]. However, due to heat transfer and cost limitations, it is difficult for these superlattices to be extended to very large energy conversion applications. Moreover, their application under high temperature is also limited. Thus, the development of new nano methods to improve the thermoelectric efficiency of TE materials is a future research topic [71].

In 1992, Hicks and Dresselhaus [72] proposed the use of lower dimensional structures to selectively modify the material properties. They theoretically proved that using two-dimensional, one-dimensional or even zero-dimensional structures can significantly improve electronic properties. Other later publications, by Venkatasubramanian [73] and Tritt [74], showed that the use of nanostructures could significantly reduce lattice thermal conductivity. Subsequently, in 1993, the nanostructure concept was used as an improvement tool to improve the material properties by Hicks and Dresselhaus [75]. Encouraged by these predictions, nanostructures and nanocomposites have been proposed and synthesized in recent years in excellent thermoelectric materials by reducing the lattice thermal conductivity. Furthermore, nanostructured materials such as quantum wells [62] (2D thermoelectric nanomaterials) and nanowires [76], nano-mesh [77] and nanoribbons [78] (1D thermoelectric nanomaterials) has been used in manufacturing novel TE devices [79]. This indicates that the ZT enhancement can be achieved in the nanometer scale or nanostructure form. Most of all, nanostructuring can improve the density of states near the Fermi level by quantum configuration, thereby providing a way of decoupling thermoelectricity and conductivity [80–82]. This may lead to a ZT value in some nanomaterials or nanostructures exceeding three [83].

Kanishka et al. [84] obtained the maximum reduction of lattice thermal conductivity by controlling and fine-tuning the mesoscale structure of nanostructured thermoelectric materials. A ZT exceeding the threshold of two was obtained at 915 K with ~2.2 ZT value. Tan et al. [16] have successfully prepared the n-type $Bi_2(Te,Se)_3$ ternary compound film composed of an ordered nanowire array by a simple thermal co-evaporation technique without using any templates. The $Bi_2(TeSe)_3$ nanowire array film has a ZT of 1.01 at room temperature. Tran and Sebastian et al. [81] proved that the natural electronic properties of

a graphene band can be fully preserved and its thermoelectric properties can be greatly improved. The room-temperature ZT of it can be enhanced from 0.26 to 2.5. These improvements in thermoelectric performance are usually made by using precise but expensive nanomaterial growth techniques. However, expensive prices are not conducive to commercialization and practical applications of thermoelectric materials are required to be inexpensive. Nanostructured composite thermoelectric materials provide the possibility to solve this problem. Nanocomposite thermoelectric material refers to a thermoelectric material doped with impurities, such as nanoparticles or nanometer-sized hollow [23]. It is considered to be a promising method for the preparation of thermoelectric materials with a high ZT value. Compared with the quantum well, quantum wire can improve the density of states. Theoretically, nanowires may have better thermoelectric properties than superlattices [30]. If the diameter of the quantum wire is less than 10 nm, the ZT value of the material may be greater than 10. Ibáñez et al. [85] suggested mixing semiconductor nanocrystals with metal nanocrystals to form ohmic contacts with bulk semiconductors. The improvements of PbS–Ag nanocomposites enhance the transport properties and increase the ZT value up to 1.7 at 850 K.

3.2. Structure/Geometry

It was found that for the designed TE module, there is an optimal length ratio to the TE module to produce a maximum output, which depends not only on the material, but also on the geometrical structure. Therefore, except for improving the thermoelectric performance by enhancing the thermoelectric materials, thermoelectric performance can also be improved by improving the structure/geometry of thermoelectric components [11,36], such as the thermoelement length [86], the number of thermocouples [87], the ratio of thermocouple length to cross-sectional area [88,89], slenderness ratio ($X = (A_p/L_p)/(A_n/L_n)$ [86,90–92] and the thermoelement with a special sectional area [93,94].

Meng et al. [95] found that the logarithm and the leg length of the TE module have a significant influence on the thermoelectric power generator (TEG) performance. The optimization of these parameters improves the performance of the TE module by 893% compared with the original design for which Zhang et al. [96] proved the geometric optimization of the thermoelectric leg played a crucial role in improving the performance of the TE module. Ferreira and Pereira [97] used the COMSOL Multiphysics software to optimize thermoelement physical dimensions. Similarly, for thermoelectric refrigeration it was found that the cooling capacity is dependent on thermoelement length, and with the reduction of the length of the thermoelectric element, this trend is becoming more and more significant. Furthermore, cooling power increases with the decrease in the ratio of thermocouple length [98]. If the thermoelement is constant, shorter thermoelement length leads to a larger cooling capacity [99]. Most commercial thermoelectric modules have thermoelectric elements ranging in length from 1.0×10^{-3} m to 2.5×10^{-3} m.

A typical thermoelectric module primarily consists of n-type and p-type TE materials fabricated from bulk thermoelectric materials, and the basic structure of it is plate-like shapes as illustrated in Figure 3.

However, due to the limited planes or angle shapes of devices such as round, cylinder and curved surfaces, device engineering has been ignored. Considering that the most of heat source surfaces connected by these planar devices are curved, there will inevitably be a lot of heat loss. It has been pointed out that the heat sources of TE generators are mostly irregular and the traditional plane structure TE device composed of vertical blocks cannot achieve ideal contact. Hence, developing novel thermoelectric module shapes or a flexible thermoelectric module is a good way to address this issue. Great efforts have been made to this end.

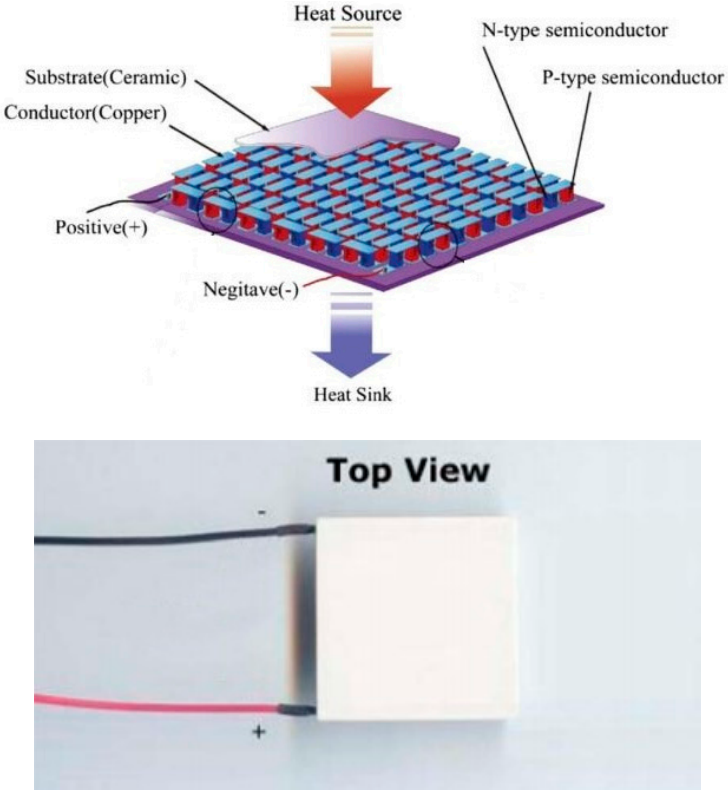


Figure 3. A typical thermoelectric module. Reproduced from [100].

A thin film thermoelectric module is an invention to overcome this technical problem. It is a thin film TEG based on a flexible fiber substrate. Film modules produced by screen printing are mentioned in [101]. Another invention to overcome this technical problem is the flexible thermoelectric material for wearable applications [102]. With the increasing popularity of 3D printing technology, flexible and bendable TE modules produced by 3D printing are gradually emerging [103]. The printable TE module will greatly improve its applicability [104].

Park et al. [105] shows a shape-engineering thermoelectric painting that is geometrically compatible with surfaces of any shape, as shown in Figure 4. They used Sb_2Te_3 thiocyanate as the sintering assistant of thermoelectric particles to prepare Bi_2Te_3-based inorganic coating. The ZT values of the n-type was 0.67 and the p-type painted materials was 1.21, which was in competition with the bulk values. The output of the TE module directly brushed on the curved surfaces was up to 4.0 mW cm^{-2}. This method paved the method for the design of a TE module that could be easily applied in more fields. It is a very promising way to make the technology be applied to where there is excess heat without limiting the shape.

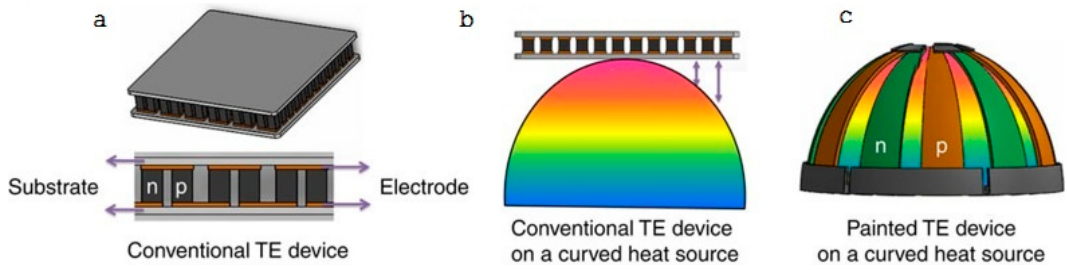


Figure 4. Traditional plane structure thermoelectric (TE) module and the bending heat source TE module. (**a**) Traditional planar TE devices. (**b**) The power generation scheme of traditional TE generator on bending heat source. (**c**) Power generation scheme of paint TE generator on bending heat source. Reproduced from [105].

3.3. Summary

Thermoelectric research has made great progress in the past 20 years. A promising way to achieve high-efficiency thermoelectric performance is to build low-dimensional nanostructures and improve the structure/geometry of the thermoelectric module. The ZT value has long surpassed once a longtime barrier value of one and great efforts were made to break through the threshold of ZT ~2. Although high ZT > 2 has been reported in low dimensional TE materials in the laboratory, many of these materials are impractical for applications due to the cost and strict manufacturing conditions. Therefore, it is urgent to develop high-performance TE modules for wider use. Furthermore, the optimization of the structure or geometry of the TE modules based on the material which is cheaper and with a ZT value that is not high is another promising way to improve their performance. In some practical cases, the TEG performance can be increased by 20–210% and the TEC performance can be increased by 10–624%. In addition, with the further development of thermoelectric technology and commercialization beyond the niche market, other factors such as the availability, life cycle, cost, as well as the manufacture of convenience should be paid more attention to in future studies.

4. Optimization of Thermal Management System of Thermoelectric Modules

According to Equation (2), the efficiency of ideal thermoelectric devices (ΔT) depends on its working temperature and the ZT value of the materials. Thus, apart from improving the thermoelectric materials, one of the key factors improving the performance of the TE modules is producing a significant temperature difference on the thermoelectric device with a certain heat flux. One way to generate a larger temperature difference is using heat exchangers on the thermoelectric modules, whose purpose is to increase the cooling at the cold end. Besides, these exchangers could reduce the thermal resistances between the TE module and the cold source or heat source. Thus, the maximum temperature difference of TE can be obtained. At the same time, different heat exchangers can be used by TE modules. This is to reduce the cost of the whole system, facilitate manufacturing and installation and improve efficiency [106,107].

4.1. Finned Heat Sink

Finned heat sinks are the most frequently used heat exchangers to improve the heat transfer on the hot side of the thermoelectric modules because of its simple structure and low cost [98]. It has been applied to many thermoelectric devices where there is no need to increase the electrical efficiency past a certain extent considering its cost. The convection coefficient will be effectively improved by enhancing the heat transfer associated with the internal flow through the pumps. Obviously, any enhancement the heat transfer coefficient usually leads to will produce an increase in the pressure losses, which in turn leads to a higher power consumption [108].

Plate fins are placed at the hot end of the semiconductor cooling plate, and the upper end uses a small fan for forced convection heat, which is shown in Figure 5. The advantages of this radiator system are simple, small footprint, low cost, representing the hot end cooling solution of most electronic devices in the current market. The disadvantages of the radiator are large thermal resistance, low convective heat transfer coefficient on the surface and high temperature at the hot end, which leads to low cooling efficiency [109].

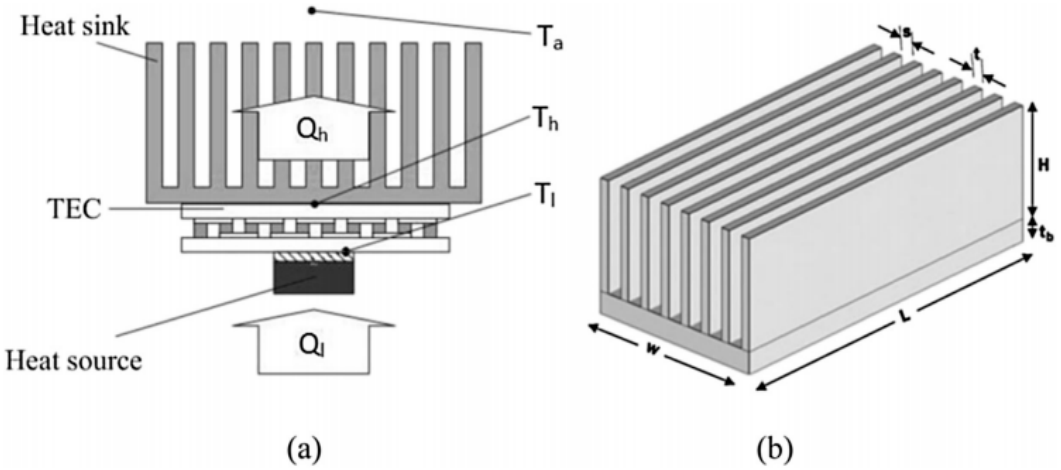


Figure 5. (**a**) The diagram of a thermoelectric cooler with a heat sink. (**b**) Structure of finned heat sink. Reproduced from [110].

The finned heat sink is widely used in many fields [111,112], such as the studied waste heat recovery of the solar system using TE modules. The finned heat sink is used for cooling the cold side of TE modules by natural convection air. [113–118] proposed thermoelectric derives to get energy from the waste heat of electronic equipment, like high-power LEDs or vehicles. In addition, the TE modules were cooled by a finned heat sink or finned heat sink with fan. In additional, many studied have sought to optimize and enhance the fined heat sink, which includes the investigation of heat sinks' geometry, different area aspect ratios and the flat metal base [119–121]. Thus, as an active cooling system, these simple finned heat sink systems can reach relatively high cooling power rates for both refrigerators and power generators [122].

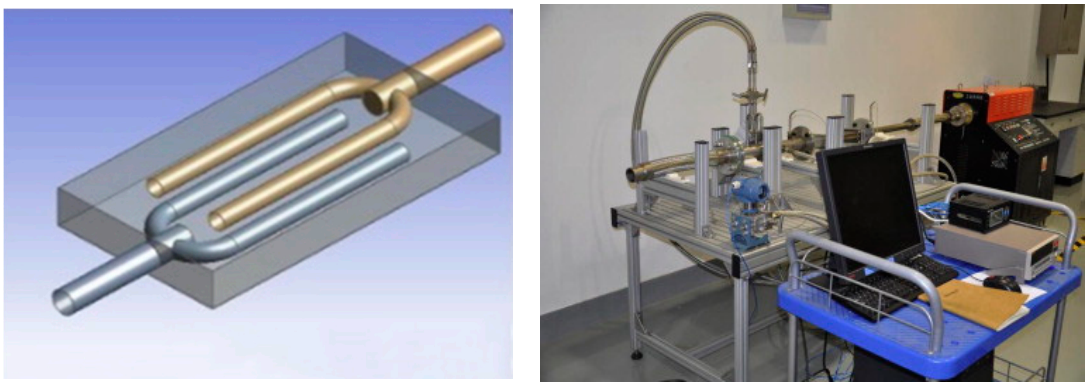
However, a air-cooled finned heat sink is sometimes not powerful enough to obtain the cooling demand (forced convection by fan, e.g., thermal resistances of 0.54–0.66 K/W and 0.5 K/W [123]). Moreover, the connection to the fins generates a higher thermal resistance (0.54–0.66 K/W), mainly because of the constriction coefficient between the finned heat sink and the TE modules as well as the low heat capacity of air. Thus, more effective heat sinks are needed [124].

4.2. Fluid–Air

The finned heat sink is the most frequently used and cheapest heat sink, but is sometimes inadequate in terms of the desired performance. Compared to the air heat exchanger, another better choice is the fluid–air heat exchanger, which uses fluid to absorb the heat from the TE module. Heat is distributed to the environment through a heat exchanger with an internal channel and fan or coil. Considering the cost and specific heat, water is the most used fluid. This type of heat exchanger is more effective and has a lower thermal resistance (example thermal resistance of 0.108 K/W [125]) because the convection coefficient of the air flow is better than that of air. In general, the water–air heat exchanger is used where the heat flow rate is high or the heat flux is large, for example the cooling or waste heat harvest of a supercomputer chip or CPU [126,127], the waste heat recovery in power plants [128–130] or the waste gas treatment in engines [131–135].

In the improvement of the water–air heat exchanger, great efforts have been made including geometrical or structural improvements [136], associating forms of channels [137]. Lesage et al. [138] experimentally studied the power enhancement performance of the TE module when the flow channel of the water–air heat exchanger has been fitted with three different geometric turbulating inserts. The results show that the increase in disturbance by the turbulating inserts can maximize the power generation by 110%. Faraji and Akbarzadeh [137] proved that a specific combination of the thermoelectric module and the tightly configured liquid channel can improve power generation efficiency. Lu et al. [139] proposed a heat exchanger on an exhaust vehicle as shown in Figure 6.

The inlet-1 and outlet-2 increased the hydraulic disturbance and lead to the enhancement of the heat transfer coefficient, making the flow distribution more uniform and the surface temperature higher than in the other two cases.



(**a**) (**b**)

Figure 6. (**a**) The internal structures of the thermoelectric power generator (TEG) heat exchanger designed by Lu et al. [139]; (**b**) the test bench.

In addition, to change the fluid refrigerant is also a direction to enhance the heat transfer. Hasan Nia et al. [140] experimentally investigated the performance of an electrical power and heat water cogeneration system by thermoelectric modules. The waste oil was used as the working fluid of the heat exchanger on the hot side of the TEG. The results show that the output power of the matched load was 1.08 W, and the efficiency was 51.33% when the radiation intensity was 705.9 W/m^2. Recently, heat exchangers with nano-fluid have shown a good ability to improve the heat transfer coefficient [141,142]. Mohammadian and Zhang [143] used Al_2O_3-water nanofluids as the working fluids to dissipate heat at the ends of the thermoelectric module. The results show that the performance coefficient of the thermoelectric module was significantly improved and the total entropy production was reduced by adding nanoparticles into the heat exchanger. Ahammed et al. [144] have studied the analysis of mixed nano-fluids in a two-channel and multiport microchannel coupled with a thermoelectric cooler. However, it still has some shortcomings. For example: although these systems can provide an improved thermal resistance, the auxiliary equipment will consume more power due to the high-convection coefficient realized by the fluid [108]. Considering that the goal is to reduce the energy consumption and make the devices more competitive, the power consumption of the auxiliary devices should be considered. Therefore, it is uncertain whether the fluid–air heat exchanger can really improve the efficiency due to the possible use of the auxiliary device.

4.3. Heat Exchangers with Phase Change

From the last sections we know that the advantages of the above two types of heat exchanger, but they cannot reach high cooling power rates as mentioned in the last section. Other types of heat exchangers are based on liquid, such as water, oil, and nano-fluid [143,144]. In these cases, auxiliary consumption exists because auxiliary equipment needs to be supplied. Nowadays, because of the latent heat, the heat exchanger with phase change has been studied in depth, which improves more heat transfer and has a smaller temperature drop 1 [145]. The heat pipe is one of the high-efficiency heat transfer devices, which transfers large amounts of heat by working fluids [146]. Moreover, the heat pipe has no moving parts and transmits a large amount of heat without any power input. According to the literature [118], the heat pipe dissipator is the best heat exchanger of medium temperature below 300 °C for TE devices.

A variety of applications and optimization methods for the heat pipe have been adopted. Zhang et al. [147] proposed an efficient, economical and practical solar thermoelectric cogenerator system using heat pipe heat exchanger to transfer and dissipate heat. Aranguren et al. [148] compared

two different types of studied heat exchangers, finned heat sinks and heat pipe heat exchangers, a TE module with two different heat exchangers. The results showed that the thermoelectric device with a heat pipe heat exchanger has a higher output performance than the thermoelectric device with fins in the same conditions, 43%. Astrain et al. [108] made a comparative study of different heat exchange systems (including finned heat sink, heat pipe and water tube) in a thermoelectric cooler as is shown in Figure 7, and it was found that the heat pipe heat exchanger was very functional in a compact space.

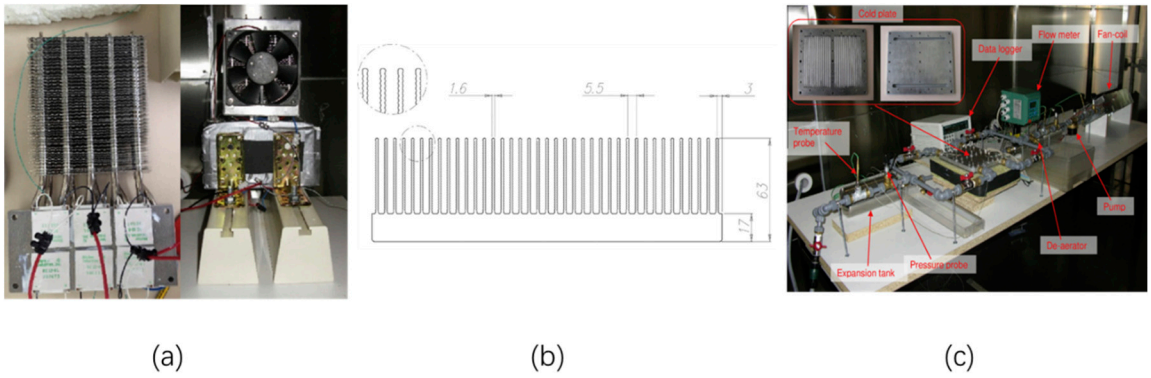


Figure 7. (**a**) Prototype of the heat pipe heat exchanger, (**b**) and the prototype of the finned heat sink. (**c**) Prototype of a water–air heat exchanger. Reproduced from [108].

Besides, the heat sink integrated with a heat pipe is a common cooling technology, and the cooling technology based on the integration of the heat sink with the thermosyphon or phase change material is also attractive. Astrain et al. [149] proposed a heat exchanger for the cold side of the TE module in thermoelectric refrigeration based on the principle of thermosyphon with phase change and capillary. After the experimental test and analysis calculation, it was found that the COP of the thermoelectric cooler with TPM (phase-change device) was 32% better than that of the COP when the finned heat sink was used. Araiz et al. [150] proposed a thermosyphon heat exchanger at the cold side of TEGs to improve their performance, as is shown in Figure 8. The net power output can be increased by 6%, which is 36% higher than the net power generation with finned heat sinks.

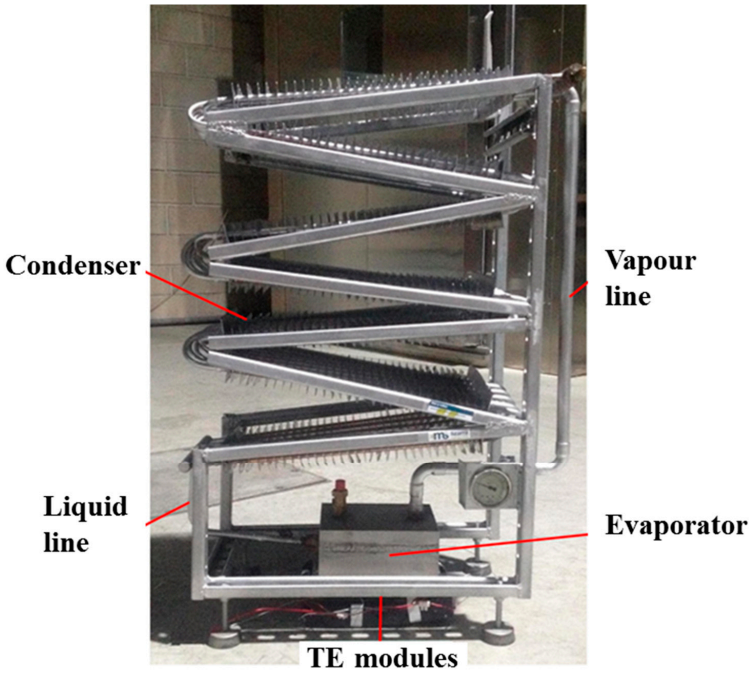


Figure 8. Prototype of the thermosyphon heat exchanger. Reproduced from [150].

4.4. Summary

One of the promising methods expected to improve TE performance is by enhancing the heat dissipation by using better heat dissipation. The chapter focuses more on the classification and improvement of the TE heat exchanger. According to the research works discussed in this section, it is summarized as follows:

Firstly, the heat exchangers applied to the TE module depend on the applications of power density. In general, forced cooling is required when the heat flux of the electronic device is greater than 0.08 W/cm^2 or the volumetric power density is greater than 0.18 W/cm^3. When the heat flux of the device is greater, large specific heat capacity fluid and other cooling methods are needed to dissipate the heat [107,119,144,145]. Secondly, the thermal design of the cooling system should depend on the inherent efficiency of the TE module, which includes the research on the heat transfer coefficients of heat exchangers on the TE module, contact thermal resistances and interface layer analysis. This study found that by inserting spiral inserts in the flow channels, the power generation can be increased by up to 110% [138]. Thirdly, as long as there is no auxiliary power consumption, another method improving the output efficiency is to use more effective heat exchangers. The over-all heat exchanger coefficient of the finned heat sink is 0.25 W/K to 0.164 W/K, for fluid–air is 1.094 W/K to 3.88 W/K, and for heat pipe is 1.72 W/K to 10.7 W/K [107,120,151]. Sinks such as the heat sink are integrated with a thermo-syphon. A last but not least method involves changing the working condition of the thermoelectric heat sink, that is, the working fluid of the heat sink and the coolant's mass flow rate, etc.

5. Extrinsic Factors: Contact Resistance

In some practical applications, the contact plates on both sides of the TE module form an interface between the surrounding and its TE components, which produced thermal contact resistance. Moreover, the performance of a TE module depends not only on the thermal management system and operating conditions, but also on the contact resistance. Actually, for practical applications, other than the thermal resistance of heat exchangers or the system itself, the existence of contact resistance makes the effective value of the thermoelectric power generation device far lower than the thermoelectricity value of the material, which greatly restricts the performance of thermoelectric power generation devices which is principally because the thermal resistance leads to a loss of temperature gradient between the TE materials, resulting in the declining of output power [152].

When considering the electrical and the contact thermal resistance, the performance of the TE module is determined by the equivalent thermoelectric zt, namely.

$$\mathrm{zt} = ZT\left(\frac{L}{L + 2\rho_c\sigma}\right) \tag{6}$$

where L is the device leg length, ρ_c is the specific contact resistivity, σ is the bulk material electrical conductivity, and zt is the material figure-of-merit. As seen in Equation (1), the specific contact resistivity ρ_c and σ significantly limits the ZT. Therefore, the performance of the TE module can be significantly improved by reducing the contact resistivity.

The contact thermal resistance would be divided into three broad categories: the contact thermal resistance between the TE module and the heat source and between the TE module and the heat sink, or caused by the TE module itself. Firstly, the contact surface is uneven, as shown in Figure 9, as an "air gap" appears in the uneven interface. These places have a large thermal resistance because of the low thermal conductivity of air.

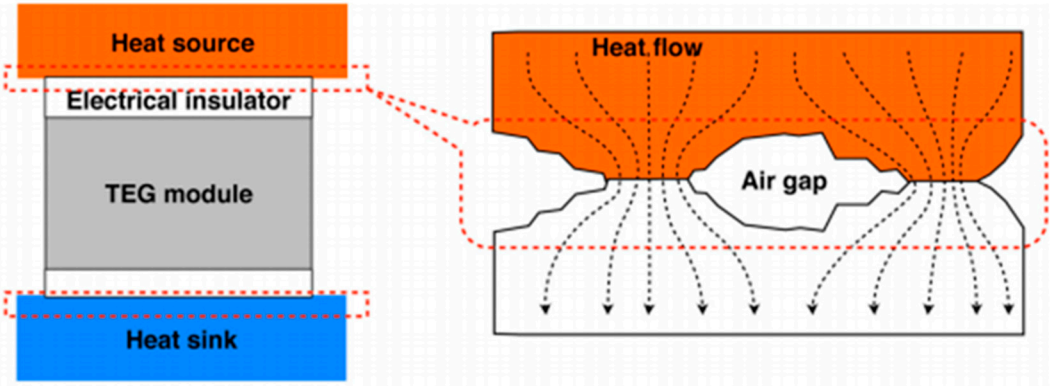


Figure 9. Schematic illustration of the thermal contact at the interface. Reproduced from [153].

Secondly, the ceramic substrates acting as electrical insulators of the TE module also cause some thermal resistance, as is shown in Figure 10. The thermal gradient $\Delta T' = (T'_H - T'_C)$ applied on both sides of the TE module is greater than $\Delta T = (T_H - T_C)$ at both ends of the p-type and n-type TE components due to the contact thermal resistance [154].

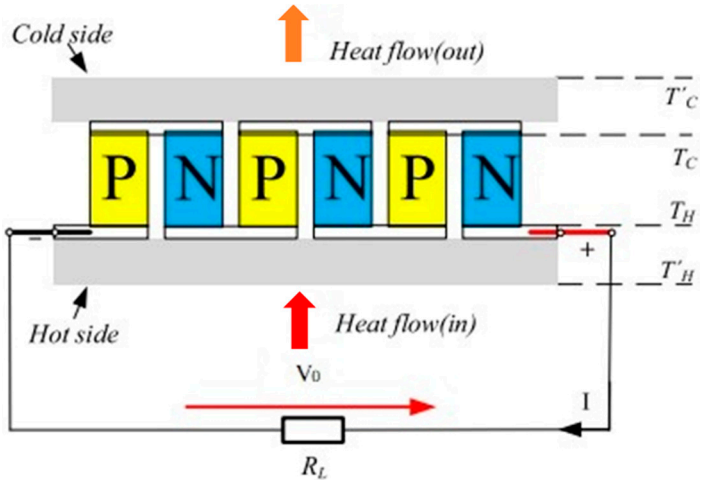


Figure 10. Schematic illustration of the thermal contact produced by the ceramic substrates. Reproduced from [155].

Thirdly, other than the thermal resistance of heat exchangers, the connection mode and processing technology between the TE module and the heat/cold source would cause an increase in thermal resistance.

The contact resistance is mainly controlled by three factors, namely heat, force and material. The other influencing factors include contact pressure, surface roughness, contact surface temperature and material properties. A great deal of work has been widely carried out to investigate the effect of contact thermal resistance on TE devices. Simulation is the most commonly used method. Many electrical and thermodynamic models have been built to accurately calculate contact resistances and analyze their influence on the performance of the TE module. BJØRK [156] has established an analytical model which can analyze the influence of contact thermal resistance. When the hot side temperature approached the peak ZT temperature and the cold side temperature remains constant at indoor temperature, the corresponding efficiency of the different thermoelectric material without contact resistance ranged from 6.88% to 14.32%. Siouane et al. [155] proposed the fully TE module with contact thermal resistance and proved that the performance of the TE module involved not only the operating conditions but also the thermal contact resistance. Luo and Kim [157] described the causes and influencing factors of contact resistance in the process of optimizing the performance of thermoelectric devices by considering the contact resistance of thermoelectric devices, and pointed

out that the existence of contact thermal resistance seriously restricted the performance of the temperature generator. Wang et al. [154] investigated the influence of the thermal contact resistance on TE performance by experiment. They demonstrated that the performance of a TE device can be significantly improved by reducing the contact thermal resistance.

Actually, for some practical applications, in order to improve the TE devices' performance, many methods have been used to reduce the contact thermal resistance. The most frequently used method is to sandwich a material with high thermal conductivity between the TE module and the heat source for decreasing their thermal contact resistance [158]. In addition, the thermal grease and conductive adhesive are often used to decrease the thermal resistance of two contact surfaces. It is the same as for a thermal adhesive, as the use of a high thermal conductivity is an effective way to reduce thermal contact resistance. The performance of the TEG has been significantly improved by reducing the contact resistance at the thermal interface [159–161].

Nowadays, more suitable thermal interface materials (TIM) are used to improve the operation performance of TE modules in different locations and working conditions. These include inorganic compounds [162], greases [163], graphite [164], metal nanometer material [165], and carbon materials. The results [153] showed that the boron nitride-based ceramic coating, white coating and polyurethane-based sheet are suitable for reducing contact resistance, respectively. The thermal resistance decreases and leads to the increase in temperature r by between 13% and 15%. In addition, close physical contact between contact surfaces is essential to minimize heat losses at the interface. This kind of contact plays an increasingly prominent role in the heat-energy collection of curvy surfaces' heat sources. However, conventional TE modules based on hard and brittle ceramic substrates are not viable for applications where surface irregularities or irregular surface shapes.

The development of highly flexible and stretchable thermoelectric modules that are pliable to curvy and deformable surfaces are urgently needed. This challenge has driven the advent of flexible and stretchable TE modules in recent decades, which created a wide range of revolutionary functional TE devices including the liquid alloy [166], silk-fabric [167] as well as printed [168] and printing technologies [169]. The manufacturing is realized by the customized layer-by-layer manufacturing process where some special methods are used to reduce the contact thermal resistance. Karwa et al. [170] designed an on-line restriction injection array heat sink in which the coolant was directly impinging on the thermoelectric module to reduce the thermal resistance of the interface. The experimental and simulation results show that a low thermal resistance 0.025 K/W can be obtained.

6. Conclusions and Further Research Direction

Considering today's energy and environmental crisis, thermoelectric modules are an application with good prospects for thermoelectric generation and thermoelectric cooling in the future. Due to the low thermoelectric conversion rate, it is still urgent to improve thermoelectric modules to promote their commercialization. This paper comprehensively reviews the efforts and methods used to improve properties and enhance the performance of thermoelectrics in terms of material progress, structure/geometry, module construction, thermal management and thermal structure design. The summaries and corresponding research directions are proposed as follows:

(1) The performance of thermoelectric devices is determined by two main factors: the thermoelectric material performance and the thermal structure, which corresponds to Z and temperature T. Thus, there are two corresponding ways to achieve high-performance thermoelectrics: one is for materials, and another is thermal design and optimization.

(2) Although a high ZT has been obtained in some low dimensional thermoelectric materials such as superlattices, nanostructures, quantum dots, nanowires, and carbon nanotubes, the highest ZT of thermoelectric materials ever found at ambient temperature is 2.4 or even higher in the lab. However, many of them are not viable for large-scale commercial use at present due to their expensive materials and complex processes. Hence, developing the novel thermoelectric module shapes to order or a flexible thermoelectric module is a good way to address this issue.

The polymer-based materials and screen-printed technology whose ZT value are generally in the range of 0.1–0.4 are flexible. It is noteworthy that the shape-engineerable painted materials are geometrically compatible to any shape. Although they do not have such a high ZT value, they are still very promising in TE applications and they also afford a new study direction for them.

(3) Compared to improving materials to enhance the figure of merit Z through complex technical means and expensive instruments, controlling temperature T by the heat sinks or heat exchangers is much easier and has a high performance–price ratio. By optimizing the structure of the heat exchanger or using appropriate heat exchangers, the performance of the TEG will be increased from 20% to 150%, and the TEC will be upgraded from 20% to 600%, compared to the original heat exchanger.

(4) In addition, thermal resistance is also an important factor affecting performance. According to the existing analytical model, when the TE working temperature approached the peak ZT temperature, the corresponding efficiency of different thermoelectric material without contact resistance was ranging from 6.88% to 14.32%. The experiment results show that using the TIM to reduce contact thermal resistance leads to 15% of temperature rises. We are not looking for ways to obtain higher values of Z, rather, the thermal structure design is another research direction in the future to achieve greater performance gains.

With its further advances in the performance of TE modules by materials and thermal structure, the future of TE devices looks bright for green energy solutions to relieve today's energy and environmental crisis from the research area into the commercial stage.

Author Contributions: All authors have read and agreed to the published version of the manuscript.

Funding: This research was funded by [National Natural Science Foundation of China] grant number [51676144] and [Fundamental Research Funds for the Central Universities] grant number [WUT: 203105003].

Conflicts of Interest: The authors declare no conflict of interest.

References

1. Khanmohammadi, S.; Saadat-Targhi, M.; Ahmed, F.W.; Afrand, M. Potential of thermoelectric waste heat recovery in a combined geothermal, fuel cell and organic Rankine flash cycle (thermodynamic and economic evaluation). *Int. J. Hydrogen Energy* **2020**, *45*, 6934–6948. [CrossRef]
2. Selvan, K.V.; Hasan, N.; Ali, M.S.M. Methodological reviews and analyses on the emerging research trends and progresses of thermoelectric generators. *Int. J. Energy Res.* **2019**, *43*, 113–140. [CrossRef]
3. He, R.; Schierning, G.; Nielsch, K. Thermoelectric Devices: Thermoelectric Devices: A Review of Devices, Architectures, and Contact Optimization (Adv. Mater. Technol. 4/2018). *Adv. Mater. Technol.* **2018**, *3*, 1700256. [CrossRef]
4. Pourkiaei, S.M.; Ahmadi, M.H.; Sadeghzadeh, M.; Moosavi, S.; Pourfayaz, F.; Chen, L.; Pour Yazdi, M.A.; Kumar, R. Thermoelectric cooler and thermoelectric generator devices: A review of present and potential applications, modeling and materials. *Energy* **2019**, *186*, 115849. [CrossRef]
5. Rowe, D.M. *CRC Handbook of Thermoelectrics*; CRC Press: Boca Raton, FL, USA, 1995.
6. Harvesting Waste Heat to Save the Climate. Available online: http://www.i-sis.org.uk/harvestingWasteHeat.php (accessed on 3 June 2020).
7. Zhao, L.-D.; Dravid, V.P.; Kanatzidis, M.G. The panoscopic approach to high performance thermoelectrics. *Energy Environ. Sci.* **2014**, *7*, 251–268. [CrossRef]
8. Majumdar, A. Enhanced: Thermoelectricity in Semiconductor Nanostructures. *Science* **2004**, *303*, 777–778. [CrossRef]
9. Cowen, L.M.; Atoyo, J.; Carnie, M.; Baran, D.; Schroeder, B.C. Review—Organic Materials for Thermoelectric Energy Generation. *ECS J. Solid State Sci. Technol.* **2017**, *6*, N3080–N3088. [CrossRef]
10. Rojas, J.; Singh, D.; Inayat, S.B.; Sevilla, G.A.T.; Fahad, H.M.; Hussain, M.M. Review—Micro and Nano-Engineering Enabled New Generation of Thermoelectric Generator Devices and Applications. *ECS J. Solid State Sci. Technol.* **2017**, *6*, N3036–N3044. [CrossRef]

11. Siddique, A.R.M.; Mahmud, S.; Van Heyst, B. A review of the state of the science on wearable thermoelectric power generators (TEGs) and their existing challenges. *Renew. Sustain. Energy Rev.* **2017**, *73*, 730–744. [CrossRef]
12. Hasaka, M.; Aki, T.; Morimura, T.; Kondo, S.-I. Thermoelectric properties of Cu-Sn-S. *Energy Convers. Manag.* **1997**, *38*, 855–859. [CrossRef]
13. Wu, H.; Zhao, L.-D.; Zheng, F.; Wu, D.; Pei, Y.L.; Tong, X.; Kanatzidis, M.G.; He, J. Broad temperature plateau for thermoelectric figure of merit ZT>2 in phase-separated PbTe0.7S0.3. *Nat. Commun.* **2014**, *5*, 1–9. [CrossRef] [PubMed]
14. Zhang, L.; Sakamoto, J. The microstructural stability and thermoelectric properties of Mm0.9Fe3.5Co0.5Sb12-based skutterudites. *Mater. Chem. Phys.* **2013**, *138*, 601–607. [CrossRef]
15. Venkatasubramanian, R.; Siivola, E.; Colpitts, T.; O'Quinn, B. Thin-film thermoelectric devices with high room-temperature figures of merit. *Nature* **2001**, *413*, 597–602. [CrossRef] [PubMed]
16. Tan, M.; Deng, Y.; Wang, Y. Ordered structure and high thermoelectric properties of Bi2(Te,Se)3 nanowire array. *Nano Energy* **2014**, *3*, 144–151. [CrossRef]
17. Pei, Y.; Shi, X.; LaLonde, A.; Wang, H.; Chen, L.; Snyder, G.J. Convergence of electronic bands for high performance bulk thermoelectrics. *Nature* **2011**, *473*, 66–69. [CrossRef] [PubMed]
18. Kim, G.-H.; Shao, L.; Zhang, K.; Pipe, K.P. Engineered doping of organic semiconductors for enhanced thermoelectric efficiency. *Nat. Mater.* **2013**, *12*, 719–723. [CrossRef]
19. Min, G.; Rowe, D. Cooling performance of integrated thermoelectric microcooler. *Solid-state Electron.* **1999**, *43*, 923–929. [CrossRef]
20. Bulman, G.; Barletta, P.; Lewis, J.; Baldasaro, N.; Manno, M.; Bar-Cohen, A.; Yang, B. Superlattice-based thin-film thermoelectric modules with high cooling fluxes. *Nat. Commun.* **2016**, *7*, 10302. [CrossRef]
21. Chowdhury, I.; Prasher, R.; Lofgreen, K.; Chrysler, G.; Narasimhan, S.; Mahajan, R.; Koester, D.; Alley, R.; Venkatasubramanian, R. On-chip cooling by superlattice-based thin-film thermoelectrics. *Nat. Nanotechnol.* **2009**, *4*, 235–238. [CrossRef]
22. Mu, S.; Zhou, H.; Zhao, W.; He, D.; Zhu, W.; Nie, X.; Sun, Z.; Zhang, Q. High-performance YbAl3/Bi0.5Sb1.5Te3 artificially tilted multilayer thermoelectric devices via material genome engineering method. *J. Power Sources* **2019**, *430*, 193–200. [CrossRef]
23. Liu, F.; Zhou, X.; Pan, C.; Wang, L. A facile method to intimately contacted nanocomposites as thermoelectric materials: Noncovalent heterojunctions. *J. Power Sources* **2019**, *412*, 153–159. [CrossRef]
24. Cai, S.; Hao, S.; Luo, Z.-Z.; Li, X.; Hadar, I.; Bailey, T.P.; Hu, X.; Uher, C.; Hu, Y.-Y.; Wolverton, C.; et al. Discordant nature of Cd in PbSe: Off-centering and core–shell nanoscale CdSe precipitates lead to high thermoelectric performance. *Energy Environ. Sci.* **2020**, *13*, 200–211. [CrossRef]
25. Nie, G.; Li, W.; Guo, J.; Yamamoto, A.; Kimura, K.; Zhang, X.; Isaacs, E.B.; Dravid, V.; Wolverton, C.; Kanatzidis, M.G.; et al. High performance thermoelectric module through isotype bulk heterojunction engineering of skutterudite materials. *Nano Energy* **2019**, *66*, 104193. [CrossRef]
26. Queen Mary Research Online. Available online: https://qmro.qmul.ac.uk (accessed on 3 June 2020).
27. Rosi, F. Thermoelectricity and thermoelectric power generation. *Solid-State Electron.* **1968**, *11*, 833–868. [CrossRef]
28. Liu, T.; Zhao, X.; Li, J.; Liu, Z.; Liscio, F.; Milita, S.; Schroeder, B.C.; Fenwick, O. Enhanced control of self-doping in halide perovskites for improved thermoelectric performance. *Nat. Commun.* **2019**, *10*, 5750. [CrossRef]
29. Mao, L.; Yin, Y.; Zhang, Q.; Liu, G.-Q.; Wang, H.; Guo, Z.; Hu, H.; Xiao, Y.; Tan, X.; Jiang, J. Fermi-surface dynamics and high thermoelectric performance along the out-of-plane direction in n-type SnSe crystals. *Energy Environ. Sci.* **2020**, *13*, 616–621. [CrossRef]
30. Mushtaq, M.; Sattar, M.A.; Dar, S.A. Phonon phase stability, structural, mechanical, electronic, and thermoelectric properties of two new semiconducting quaternary Heusler alloys CoCuZrZ (Z = Ge and Sn). *Int. J. Energy Res.* **2020**, *44*, 5936–5946. [CrossRef]
31. He, W.; Wang, D.; Wu, H.; Xiao, Y.; Zhang, Y.; He, D.; Feng, Y.; Hao, Y.-J.; Dong, J.-F.; Chetty, R.; et al. High thermoelectric performance in low-cost SnS0.91Se0.09 crystals. *Sci.* **2019**, *365*, 1418–1424. [CrossRef]
32. You, L.; Zhang, J.; Pan, S.; Jiang, Y.; Wang, K.; Yang, J.; Pei, Y.; Zhu, Q.; Agne, M.T.; Snyder, G.J.; et al. Realization of higher thermoelectric performance by dynamic doping of copper in n-type PbTe. *Energy Environ. Sci.* **2019**, *12*, 3089–3098. [CrossRef]
33. Wang, X.; Xu, J.; Liu, G.; Fu, Y.; Tan, X.; Shao, H.; Jiang, H. Optimization of thermoelectric properties in n-type SnSe doped with BiCl3. *Appl. Phys. Lett.* **2016**, *108*, 83902. [CrossRef]

34. Mao, J.; Zhu, H.; Ding, Z.; Liu, Z.; Gamage, G.A.; Chen, G.; Ren, Z. High thermoelectric cooling performance of n-type Mg3Bi2-based materials. *Science* **2019**, *365*, 495–498. [CrossRef] [PubMed]
35. Pan, Y.; Qiu, Y.; Witting, I.; Zhang, L.; Fu, C.; Li, J.-W.; Huang, Y.; Sun, F.-H.; He, J.; Snyder, G.J.; et al. Synergistic modulation of mobility and thermal conductivity in (Bi,Sb)2Te3 towards high thermoelectric performance. *Energy Environ. Sci.* **2019**, *12*, 624–630. [CrossRef]
36. Zhu, H.; Mao, J.; Li, Y.; Sun, J.; Wang, Y.; Zhu, Q.; Li, G.; Song, Q.; Zhou, J.; Fu, Y.; et al. Discovery of TaFeSb-based half-Heuslers with high thermoelectric performance. *Nat. Commun.* **2019**, *10*, 270. [CrossRef]
37. Kim, S.I.; Lee, K.H.; A Mun, H.; Kim, H.S.; Hwang, S.W.; Roh, J.W.; Yang, D.J.; Shin, W.H.; Li, X.S.; Lee, Y.H.; et al. Dense dislocation arrays embedded in grain boundaries for high-performance bulk thermoelectrics. *Science* **2015**, *348*, 109–114. [CrossRef] [PubMed]
38. Hu, L.; Zhu, T.; Liu, X.; Zhao, X. Point Defect Engineering of High-Performance Bismuth-Telluride-Based Thermoelectric Materials. *Adv. Funct. Mater.* **2014**, *24*, 5211–5218. [CrossRef]
39. Witting, I.T.; Chasapis, T.C.; Ricci, F.; Peters, M.; Heinz, N.A.; Hautier, G.; Snyder, G.J. The Thermoelectric Properties of Bismuth Telluride. *Adv. Electron. Mater.* **2019**, *5*, 1800904. [CrossRef]
40. Shi, X.-L.; Tao, X.; Zou, J.; Chen, Z.-G. High-Performance Thermoelectric SnSe: Aqueous Synthesis, Innovations, and Challenges. *Adv. Sci.* **2020**, *7*, 1902923. [CrossRef]
41. Zhao, L.-D.; Tan, G.; Hao, S.; He, J.; Pei, Y.; Chi, H.; Wang, H.; Gong, S.; Xu, H.; Dravid, V.P.; et al. Ultrahigh power factor and thermoelectric performance in hole-doped single-crystal SnSe. *Science* **2015**, *351*, 141–144. [CrossRef]
42. Chere, E.K.; Zhang, Q.; Dahal, K.; Cao, F.; Mao, J.; Ren, Z. Studies on thermoelectric figure of merit of Na-doped p-type polycrystalline SnSe. *J. Mater. Chem. A* **2016**, *4*, 1848–1854. [CrossRef]
43. Zheng, Z.; Su, X.; Deng, R.; Stoumpos, C.C.; Xie, H.; Liu, W.; Yan, Y.; Hao, S.; Uher, C.; Wolverton, C.; et al. Rhombohedral to Cubic Conversion of GeTe via MnTe Alloying Leads to Ultralow Thermal Conductivity, Electronic Band Convergence, and High Thermoelectric Performance. *J. Am. Chem. Soc.* **2018**, *140*, 2673–2686. [CrossRef]
44. Kang, J.; Jung, D.W.; Park, S.; Lee, J.-H.; Ko, J.; Kim, J. Corrigendum to "Accelerated test analysis of reversal potential caused by fuel starvation during PEMFCs operation" [International Journal of Hydrogen Energy 35 (2010) 3727–3735]. *Int. J. Hydrogen Energy* **2010**, *35*, 8815. [CrossRef]
45. Fu, Y.; Yang, J.; Qin, H.; Shao, H.; Xu, J.; Liu, G.-Q.; Tan, X.; Jiang, H.; Liang, B. Enhanced thermoelectric performance in p-type polycrystalline SnSe benefiting from texture modulation. *J. Mater. Chem. C* **2016**, *4*, 1201–1207. [CrossRef]
46. Qin, B.; Wang, D.; He, W.; Zhang, Y.; Wu, H.; Pennycook, S.J.; Zhao, L.-D. Realizing High Thermoelectric Performance in p-Type SnSe through Crystal Structure Modification. *J. Am. Chem. Soc.* **2018**, *141*, 1141–1149. [CrossRef] [PubMed]
47. Wei, T.-R.; Tan, G.; Zhang, X.; Wu, C.-F.; Li, J.-F.; Dravid, V.P.; Snyder, G.J.; Kanatzidis, M.G. Distinct Impact of Alkali-Ion Doping on Electrical Transport Properties of Thermoelectric p-Type Polycrystalline SnSe. *J. Am. Chem. Soc.* **2016**, *138*, 8875–8882. [CrossRef] [PubMed]
48. Peng, K.; Lu, X.; Zhan, H.; Hui, S.; Tang, X.; Wang, G.; Dai, J.; Uher, C.; Wang, G.; Zhou, X. Broad temperature plateau for high ZTs in heavily doped p-type SnSe single crystals. *Energy Environ. Sci.* **2016**, *9*, 454–460. [CrossRef]
49. Tan, G.; Shi, F.; Hao, S.; Chi, H.; Zhao, L.D.; Uher, C.; Wolverton, C.; Dravid, V.P.; Kanatzidis, M.G. Codoping in SnTe: Enhancement of Thermoelectric Performance through Synergy of Resonance Levels and Band Convergence. *J. Am. Chem. Soc.* **2015**, *137*, 5100–5112. [CrossRef]
50. Yang, L.; Chen, Z.-G.; Hong, M.; Wang, L.; Kong, D.; Huang, L.; Han, G.; Zou, Y.-C.; Dargusch, M.; Zou, J. n-type Bi-doped PbTe Nanocubes with Enhanced Thermoelectric Performance. *Nano Energy* **2017**, *31*, 105–112. [CrossRef]
51. Shuai, J.; Sun, Y.; Tan, X.; Mori, T. Manipulating the Ge Vacancies and Ge Precipitates through Cr Doping for Realizing the High-Performance GeTe Thermoelectric Material. *Small* **2020**, *16*, e1906921. [CrossRef]
52. Pan, Y.; Aydemir, U.; Grovogui, J.A.; Witting, I.T.; Hanus, R.; Xu, Y.; Wu, J.; Wu, C.-F.; Sun, F.-H.; Zhuang, H.-L.; et al. Melt-Centrifuged (Bi,Sb)2 Te3: Engineering Microstructure toward High Thermoelectric Efficiency. *Adv. Mater.* **2018**, *30*, 1802016. [CrossRef]
53. Takaki, H.; Kobayashi, K.; Shimono, M.; Kobayashi, N.; Hirose, K. First-principles calculations of thermoelectric properties of TiN/MgO superlattices: The route for an enhancement of thermoelectric effects in artificial nanostructures. *J. Appl. Phys.* **2016**, *119*, 014302. [CrossRef]

54. Song, D.; Ma, W.; Zhang, X. Lattice thermal conductivity of Si/Ge composite thermoelectric material: Effect of Si particle distribution. *Int. J. Energy Res.* **2018**, *43*, 379–390. [CrossRef]
55. Niemelä, J.-P.; Karttunen, A.J.; Karppinen, M. Inorganic–organic superlattice thin films for thermoelectrics. *J. Mater. Chem. C* **2015**, *3*, 10349–10361. [CrossRef]
56. Yang, R.; Chen, G. Nanostructured thermoelectric materials: From superlattices to nanocomposites. *Mater. Integr.* **2005**, *18*, 31–36.
57. Shakouri, A. Recent Developments in Semiconductor Thermoelectric Physics and Materials. *Annu. Rev. Mater. Res.* **2011**, *41*, 399–431. [CrossRef]
58. Beyer, H.; Nurnus, J.; Böttner, H.; Lambrecht, A.; Wagner, E.; Bauer, G. High thermoelectric figure of merit ZT in PbTe and Bi2Te3-based superlattices by a reduction of the thermal conductivity. *Phys. E Low-Dimens. Syst. Nanostructures* **2002**, *13*, 965–968. [CrossRef]
59. Harman, T.C. Quantum Dot Superlattice Thermoelectric Materials and Devices. *Science* **2002**, *297*, 2229–2232. [CrossRef]
60. Lee, S.-M.; Cahill, D.G.; Venkatasubramanian, R. Thermal conductivity of Si–Ge superlattices. *Appl. Phys. Lett.* **1997**, *70*, 2957–2959. [CrossRef]
61. Zeng, G.; Shakouri, A.; LaBounty, C.; Robinson, G.; Croke, E.; Abraham, P.; Fan, X.; Reese, H.; Bowers, J. SiGe micro-cooler. *Electron. Lett.* **1999**, *35*, 2146–2147. [CrossRef]
62. Harman, T.C.; Taylor, P.J.; Spears, D.L.; Walsh, M.P. Thermoelectric quantum-dot superlattices with high ZT. *J. Electron. Mater.* **2000**, *29*, L1–L2. [CrossRef]
63. Zong, P.A.; Zhang, P.; Yin, S.; Huang, Y.; Wang, Y.; Wan, C. Fabrication and Characterization of a Hybrid Bi_2Se_3/Organic Superlattice for Thermoelectric Energy Conversion. *Adv. Electr. Mater.* **2019**, *5*, 1800842. [CrossRef]
64. Hicks, L.D.; Harman, T.C.; Sun, X.; Dresselhaus, M.S. Experimental study of the effect of quantum-well structures on the thermoelectric figure of merit. *Phys. Rev. B* **1996**, *53*, R10493–R10496. [CrossRef] [PubMed]
65. Tritt, T.M. *Thermal Conductivity: Theory, Properties, and Applications*; Springer Science & Business Media: Berlin, Germany, 2004.
66. Harman, T.C.; Walsh, M.P.; Turner, G.W. Nanostructured thermoelectric materials. *J. Electr. Mater.* **2005**, *34*, L19–L22. [CrossRef]
67. Park, N.W.; Lee, W.Y.; Yoon, Y.S.; Kim, G.S.; Yoon, Y.G.; Lee, S.K. Achieving Out-of-Plane Thermoelectric Figure of Merit ZT=1.44 in a p-Type Bi2Te3/Bi0.5Sb1.5Te3 Superlattice Film with Low Interfacial Resistance. *ACS Appl. Mater. Interfaces* **2019**, *11*, 38247–38254. [CrossRef] [PubMed]
68. Priyadarshi, P.; Sharma, A.; Mukherjee, S.; Muralidharan, B. Superlattice design for optimal thermoelectric generator performance. *J. Phys. D: Appl. Phys.* **2018**, *51*, 185301. [CrossRef]
69. Zhou, Y.; Zhao, L.-D. Promising Thermoelectric Bulk Materials with 2D Structures. *Adv. Mater.* **2017**, *29*, 1702676. [CrossRef]
70. Mamur, H.; Bhuiyan, M.R.A.; Korkmaz, F.; Nil, M. A review on bismuth telluride (Bi_2Te_3) nanostructure for thermoelectric applications. *Renew. Sustain. Energy Rev.* **2018**, *82*, 4159–4169. [CrossRef]
71. Rowe, D.M. *Thermoelectrics Handbook: Macro to Nano*; CRC Press: Boca Raton, FL, USA, 2005.
72. Hicks, L.D.; Dresselhaus, M.S. The Effect of Quantum Well Structures on the Thermoelectric Figure of Merit. *MRS Proc.* **1992**, *281*, 450–453. [CrossRef]
73. Venkatasubramanian, R. Chapter 4 Phonon blocking electron transmitting superlattice structures as advanced thin film thermoelectric materials. *Semiconduct. Semimet.* **2001**, *71*, 175–201.
74. Tritt, T.M. *Recent Trends in Thermoelectric Materials Research III*; Semiconductors and Semimetals—Preface; Academic Press: New York, NY, USA, 2001; Volume 71, pp. 9–14.
75. Hicks, L.D.; Dresselhaus, M.S. Effect of quantum-well structures on the thermoelectric figure of merit. *Phys. Rev. B* **1993**, *47*, 12727–12731. [CrossRef]
76. Boukai, A.I.; Bunimovich, Y.; Tahir-Kheli, J.; Yu, J.-K.; Iii, W.A.G.; Heath, J.R. Silicon nanowires as efficient thermoelectric materials. *Nature* **2008**, *451*, 168–171. [CrossRef]
77. Yu, J.-K.; Mitrovic, S.; Tham, D.; Varghese, J.; Heath, J.R. Reduction of thermal conductivity in phononic nanomesh structures. *Nat. Nanotechnol.* **2010**, *5*, 718–721. [CrossRef] [PubMed]
78. Sadeghi, H.; Sangtarash, S.; Lambert, C.J. Enhancing the thermoelectric figure of merit in engineered graphene nanoribbons. *Beilstein J. Nanotechnol.* **2015**, *6*, 1176–1182. [CrossRef]
79. Tang, J.; Chen, Y.; McCuskey, S.R.; Chen, L.; Bazan, G.C.; Liang, Z. Recent Advances in n-Type Thermoelectric Nanocomposites. *Adv. Electr. Mater.* **2019**, *5*, 1800943. [CrossRef]

80. Wang, J.; Zhang, B.-Y.; Kang, H.; Li, Y.; Yaer, X.; Li, J.; Tan, Q.; Zhang, S.; Fan, G.-H.; Liu, C.-Y.; et al. Record high thermoelectric performance in bulk SrTiO3 via nano-scale modulation doping. *Nano Energy* **2017**, *35*, 387–395. [CrossRef]
81. Tran, V.T.; Saint-Martin, J.; Dollfus, P.; Volz, S. Optimizing the thermoelectric performance of graphene nano-ribbons without degrading the electronic properties. *Sci. Rep.* **2017**, *7*, 2313. [CrossRef] [PubMed]
82. Hossain, S.; Huynh, D.H.; Jiang, L.; Rahman, S.; Nguyen, P.D.; Al-Dirini, F.; Hossain, F.M.; Bahk, J.-H.; Skafidas, E.; Skafidas, S. Investigating enhanced thermoelectric performance of graphene-based nano-structures. *Nanoscale* **2018**, *10*, 4786–4792. [CrossRef]
83. Li, K.-M.; Xie, Z.-X.; Su, K.-L.; Luo, W.; Zhang, Y. Ballistic thermoelectric properties in double-bend graphene nanoribbons. *Phys. Lett. A* **2014**, *378*, 1383–1387. [CrossRef]
84. Biswas, K.; He, J.; Blum, I.D.; Wu, C.I.; Hogan, T.P.; Seidman, D.N.; Dravid, V.P.; Kanatzidis, M.G. High-performance bulk thermoelectrics with all-scale hierarchical architectures. *Nature* **2012**, *489*, 414–418. [CrossRef]
85. Ibánez, M.; Luo, Z.; Genc, A.; Piveteau, L.; Ortega, S.; Cadavid, D.; Dobrozhan, O.; Liu, Y.; Nachtegaal, M.; Zebarjadi, M.; et al. High-performance thermoelectric nanocomposites from nanocrystal building blocks. *Nat. Commun.* **2016**, *7*, 10766. [CrossRef]
86. Karana, D.R.; Sahoo, R.R. Influence of geometric parameter on the performance of a new asymmetrical and segmented thermoelectric generator. *Energy* **2019**, *179*, 90–99. [CrossRef]
87. Chen, J.; Li, K.; Liu, C.; Li, M.; Lv, Y.; Jia, L.; Jiang, S. Enhanced Efficiency of Thermoelectric Generator by Optimizing Mechanical and Electrical Structures. *Energies* **2017**, *10*, 1329. [CrossRef]
88. Lv, S.; Liu, M.; He, W.; Li, X.; Gong, W.; Shen, S. Study of thermal insulation materials influence on the performance of thermoelectric generators by creating a significant effective temperature difference. *Energy Convers. Manag.* **2020**, *207*, 112516. [CrossRef]
89. Lundgaard, C.; Sigmund, O.; Bjørk, R. Topology Optimization of Segmented Thermoelectric Generators. *J. Electron. Mater.* **2018**, *47*, 6959–6971. [CrossRef]
90. Wang, X.; Wang, H.; Su, W.; Mehmood, F.; Zhai, J.; Wang, T.; Chen, T.; Wang, C. Geometric structural design for lead tellurium thermoelectric power generation application. *Renew. Energy* **2019**, *141*, 88–95. [CrossRef]
91. Ali, H.; Yilbas, B.S.; Al-Sharafi, A. Segmented thermoelectric generator: Exponential area variation in leg. *Int. J. Energy Res.* **2018**, *42*, 477–489. [CrossRef]
92. Ming, T.; Yang, W.; Wu, Y.; Xiang, Y.; Huang, X.; Cheng, J.; Li, X.; Zhao, J. Numerical analysis on the thermal behavior of a segmented thermoelectric generator. *Int. J. Hydrogen Energy* **2017**, *42*, 3521–3535. [CrossRef]
93. Sun, H.; Ge, Y.; Liu, W.; Liu, Z. Geometric optimization of two-stage thermoelectric generator using genetic algorithms and thermodynamic analysis. *Energy* **2019**, *171*, 37–48. [CrossRef]
94. Shittu, S.; Li, G.; Zhao, X.; Ma, X.; Akhlaghi, Y.G.; Ayodele, E. Optimized high performance thermoelectric generator with combined segmented and asymmetrical legs under pulsed heat input power. *J. Power Sources* **2019**, *428*, 53–66. [CrossRef]
95. Meng, J.-H.; Zhang, X.; Wang, X.-D. Multi-objective and multi-parameter optimization of a thermoelectric generator module. *Energy* **2014**, *71*, 367–376. [CrossRef]
96. Zhang, A.; Wang, B.; Pang, D.; Chen, J.; Wang, J.; Du, J. Influence of leg geometry configuration and contact resistance on the performance of annular thermoelectric generators. *Energy Convers. Manag.* **2018**, *166*, 337–342. [CrossRef]
97. Teixeira, S.F.; Pereira, A.M. Geometrical optimization of a thermoelectric device: Numerical simulations. *Energy Convers. Manag.* **2018**, *169*, 217–227. [CrossRef]
98. Zhao, D.; Tan, G. A review of thermoelectric cooling: Materials, modeling and applications. *Appl. Therm. Eng.* **2014**, *66*, 15–24. [CrossRef]
99. Badillo-Ruiz, C.A.; Olivares-Robles, M.A.; Ortega, P.E.R. Performance of Segmented Thermoelectric Cooler Micro-Elements with Different Geometric Shapes and Temperature-Dependent Properties. *Entropy* **2018**, *20*, 118. [CrossRef]
100. Tzeng, S.C.; Jeng, T.M.; Lin, Y.L. Parametric study of heat-transfer design on the thermoelectric generator system. *Int. Commun. Heat Mass Transf.* **2014**, *52*, 97–105. [CrossRef]
101. Lee, H.-B.; Yang, H.J.; We, J.H.; Kim, K.; Choi, K.C.; Cho, B.J. Thin-Film Thermoelectric Module for Power Generator Applications Using a Screen-Printing Method. *J. Electron. Mater.* **2011**, *40*, 615–619. [CrossRef]
102. Bahk, J.-H.; Fang, H.; Yazawa, K.; Shakouri, A. Flexible thermoelectric materials and device optimization for wearable energy harvesting. *J. Mater. Chem. C* **2015**, *3*, 10362–10374. [CrossRef]

103. Kim, F.; Kwon, B.; Eom, Y.; Lee, J.E.; Park, S.; Jo, S.; Park, S.H.; Kim, B.S.; Im, H.J.; Lee, M.H.; et al. 3D printing of shape-conformable thermoelectric materials using all-inorganic Bi2Te3-based inks. *Nat. Commun.* **2018**, *3*, 301–309. [CrossRef]
104. Huu, T.N.; Van, T.N.; Takahito, O. Flexible thermoelectric power generator with Y-type structure using electrochemical deposition process. *Appl. Energy* **2018**, *210*, 467–476. [CrossRef]
105. Park, S.H.; Jo, S.; Kwon, B.; Kim, F.; Ban, H.W.; Lee, J.E.; Gu, D.H.; Lee, S.H.; Hwang, Y.; Kim, J.-S.; et al. High-performance shape-engineerable thermoelectric painting. *Nat. Commun.* **2016**, *7*, 13403. [CrossRef] [PubMed]
106. Hwang, J.; Kim, H.; Wijethunge, D.; Nandihalli, N.; Eom, Y.; Park, H.; Kim, J.; Kim, W. More than half reduction in price per watt of thermoelectric device without increasing the thermoelectric figure of merit of materials. *Appl. Energy* **2017**, *205*, 1459–1466. [CrossRef]
107. Elghool, A.; Basrawi, F.; Ibrahim, T.K.; Habib, K.; Ibrahim, H.; Idris, D.M.N.D. A review on heat sink for thermo-electric power generation: Classifications and parameters affecting performance. *Energy Convers. Manag.* **2017**, *134*, 260–277. [CrossRef]
108. Astrain, D.; Aranguren, P.; Martinez, A.; Rodríguez, A.; Pérez-Artieda, G. A comparative study of different heat exchange systems in a thermoelectric refrigerator and their influence on the efficiency. *Appl. Therm. Eng.* **2016**, *103*, 1289–1298. [CrossRef]
109. Wang, T.; Ma, S. Thermoelectric generator heat performance study about improved fin structures. *Therm. Sci.* **2018**, *22*, 101–112. [CrossRef]
110. Sarkar, A.; Mahapatra, S.K. Role of surface radiation on the functionality of thermoelectric cooler with heat sink. *Appl. Therm. Eng.* **2014**, *69*, 39–45. [CrossRef]
111. Xiao, L.; Wu, S.Y.; Yang, S.L. Parametric study on the thermoelectric conversion performance of a concentrated solar-driven thermionic-thermoelectric hybrid generator. *Int. J. Energy Res.* **2018**, *42*, 656–672. [CrossRef]
112. Al-Nimr, M.D.A.; Qananba, K.S. A solar hybrid thermoelectric generator and distillation system. *Int. J. Green Energy* **2018**, *15*, 473–488. [CrossRef]
113. Wang, J.; Cai, Y.-X.; Bao, W.; Li, H.-X.; Liu, Q. Experimental study of high power LEDs heat dissipation based on corona discharge. *Appl. Therm. Eng.* **2016**, *98*, 420–429. [CrossRef]
114. Najjar, Y.S.H.; Kseibi, M. Evaluation of experimental JUST thermoelectric stove for electricity—Deprived regions. *Renew. Sustain. Energy Rev.* **2017**, *69*, 854–861. [CrossRef]
115. Tsai, H.-L.; Le, P.T. Self-sufficient energy recycling of light emitter diode/thermoelectric generator module for its active-cooling application. *Energy Convers. Manag.* **2016**, *118*, 170–178. [CrossRef]
116. Khalil, H.; Hassan, H. Enhancement thermoelectric generators output power from heat recovery of chimneys by using flaps. *J. Power Sources* **2019**, *443*, 227266. [CrossRef]
117. Patowary, R.; Baruah, D.C. Thermoelectric conversion of waste heat from IC engine-driven vehicles: A review of its application, issues, and solutions. *Int. J. Energy Res.* **2018**, *42*, 2595–2614. [CrossRef]
118. Mirhosseini, M.; Rezania, A.; Rosendahl, L.A. Power optimization and economic evaluation of thermoelectric waste heat recovery system around a rotary cement kiln. *J. Clean. Prod.* **2019**, *232*, 1321–1334. [CrossRef]
119. Ong, K.S.; Tan, C.; Lai, K.; Tan, K. Heat spreading and heat transfer coefficient with fin heat sink. *Appl. Therm. Eng.* **2017**, *112*, 1638–1647. [CrossRef]
120. Lv, S.; He, W.; Hu, D.; Zhu, J.; Li, G.; Chen, H.; Liu, M. Study on a high-performance solar thermoelectric system for combined heat and power. *Energy Convers. Manag.* **2017**, *143*, 459–469. [CrossRef]
121. Lv, S.; He, W.; Jiang, Q.; Hu, Z.; Liu, X.; Chen, H.; Liu, M. Study of different heat exchange technologies influence on the performance of thermoelectric generators. *Energy Convers. Manag.* **2018**, *156*, 167–177. [CrossRef]
122. Martínez, A.; Astrain, D.; Aranguren, P. Thermoelectric self-cooling for power electronics: Increasing the cooling power. *Energy* **2016**, *112*, 1–7. [CrossRef]
123. Chang, Y.-W.; Chang, C.-C.; Ke, M.-T.; Chen, S.-L. Thermoelectric air-cooling module for electronic devices. *Appl. Therm. Eng.* **2009**, *29*, 2731–2737. [CrossRef]
124. Alghoul, M.; Shahahmadi, S.A.; Yeganeh, B.; Asim, N.; Elbreki, A.; Sopian, K.; Tiong, S.; Amin, N. A review of thermoelectric power generation systems: Roles of existing test rigs/ prototypes and their associated cooling units on output performance. *Energy Convers. Manag.* **2018**, *174*, 138–156. [CrossRef]
125. Huang, H.-S.; Weng, Y.-C.; Chang, Y.-W.; Chen, S.-L.; Ke, M.-T. Thermoelectric water-cooling device applied to electronic equipment. *Int. Commun. Heat Mass Transf.* **2010**, *37*, 140–146. [CrossRef]
126. Wiriyasart, S.; Hommalee, C.; Naphon, P. Thermal cooling enhancement of dual processors computer with thermoelectric air cooler module. *CASE Stud. Therm. Eng.* **2019**, *14*, 10045. [CrossRef]

127. Hu, H.; Ge, T.; Dai, Y.; Wang, R. Experimental study on water-cooled thermoelectric cooler for CPU under severe environment. *Int. J. Refrig.* **2016**, *62*, 30–38. [CrossRef]
128. Meng, F.; Chen, L.; Sun, F.; Yang, B. Thermoelectric power generation driven by blast furnace slag flushing water. *Energy* **2014**, *66*, 965–972. [CrossRef]
129. Li, W.; Peng, J.; Xiao, W.; Wang, H.; Zeng, J.; Xie, J.; Huang, Q.; Mao, K.; Zhang, L. The temperature distribution and electrical performance of fluid heat exchanger-based thermoelectric generator. *Appl. Therm. Eng.* **2017**, *118*, 742–747. [CrossRef]
130. Junior, M.F.; Bezerra, U.H.; Leite, J.C.; Moya-Rodríguez, J.L. Maintenance Tools applied to Electric Generators to Improve Energy Efficiency and Power Quality of Thermoelectric Power Plants. *Energies* **2017**, *10*, 1091. [CrossRef]
131. Shixue, H.W.W. Performance Comparison of Different Exhaust Exchanger Types Considering Peak Net Power and Optimal Dimension in a Thermoelectric Generator System. *Adv. Theory Simul.* **2018**, *1*, 1800012.
132. Xiao, G.Q.; Zhang, Z. Coupled simulation of a thermoelectric generator of a thermoelectric generator applied in diesel engine exhaust waste heat recovery. *Therm. Sci.* **2020**, *24*, 281–292. [CrossRef]
133. Zhao, Y.; Wang, S.; Ge, M.; Li, Y.; Liang, Z.; Yang, Y. Performance analysis of a thermoelectric generator applied to wet flue gas waste heat recovery. *Appl. Energy* **2018**, *228*, 2080–2089. [CrossRef]
134. Meng, F.; Chen, L.; Feng, Y.; Xiong, B. Thermoelectric generator for industrial gas phase waste heat recovery. *Energy* **2017**, *135*, 83–90. [CrossRef]
135. Lu, B.; Meng, X.; Tian, Y.; Zhu, M.; Suzuki, R.O. Thermoelectric performance using counter-flowing thermal fluids. *Int. J. Hydrogen Energy* **2017**, *42*, 20835–20842. [CrossRef]
136. Liu, X.; Yu, J. Numerical study on performances of mini-channel heat sinks with non-uniform inlets. *Appl. Therm. Eng.* **2016**, *93*, 856–864. [CrossRef]
137. Faraji, A.Y.; Akbarzadeh, A. Analysis of a symbiotic thermoelectric system for power generation and liquid preheating. *Appl. Therm. Eng.* **2014**, *71*, 501–507. [CrossRef]
138. Lesage, F.J.; Sempels, E.; Lalande-Bertrand, N. A study on heat transfer enhancement using flow channel inserts for thermoelectric power generation. *Energy Convers. Manag.* **2013**, *75*, 532–541. [CrossRef]
139. Lu, H.; Wu, T.; Bai, S.; Xu, K.; Huang, Y.; Gao, W.; Yin, X.; Chen, L. Experiment on thermal uniformity and pressure drop of exhaust heat exchanger for automotive thermoelectric generator. *Energy* **2013**, *54*, 372–377. [CrossRef]
140. Nia, M.H.; Nejad, A.A.; Goudarzi, A.; Valizadeh, M.; Samadian, P. Cogeneration solar system using thermoelectric module and fresnel lens. *Energy Convers. Manag.* **2014**, *84*, 305–310. [CrossRef]
141. Lian, D.; Jitian, H.; Chong, H.; Linlin, C. Natural circulation heat transfer characteristics of nanofluid in thermoelectric refrigeration liquid cooling suits. *J. Southeast Univ.* **2018**, *48*, 220–225.
142. Xing, J.-J.; Wu, Z.; Xie, H.; Wang, Y.-Y.; Li, Y.-H.; Mao, J.-H. Performance of thermoelectric generator with graphene nanofluid cooling. *Chin. Phys. B* **2017**, *26*, 104401. [CrossRef]
143. Mohammadian, S.K.; Zhang, Y. Analysis of nanofluid effects on thermoelectric cooling by micro-pin-fin heat exchangers. *Appl. Therm. Eng.* **2014**, *70*, 282–290. [CrossRef]
144. Ahammed, N.; Asirvatham, L.G.; Wongwises, S. Entropy generation analysis of graphene–alumina hybrid nanofluid in multiport minichannel heat exchanger coupled with thermoelectric cooler. *Int. J. Heat Mass Transf.* **2016**, *103*, 1084–1097. [CrossRef]
145. Shabgard, H.; Allen, M.J.; Sharifi, N.; Benn, S.P.; Faghri, A.; Bergman, T.L. Heat pipe heat exchangers and heat sinks: Opportunities, challenges, applications, analysis, and state of the art. *Int. J. Heat Mass Transf.* **2015**, *89*, 138–158. [CrossRef]
146. Omer, G.; Yavuz, H.; Ahiska, R. Heat pipes thermoelectric solar collectors for energy applications. *Int. J. Hydrogen Energy* **2017**, *42*, 8310–8313. [CrossRef]
147. Zhang, M.; Miao, L.; Kang, Y.P.; Tanemura, S.; Fisher, C.A.J.; Xu, G.; Li, C.X.; Fan, G.Z. Efficient, low-cost solar thermoelectric cogenerators comprising evacuated tubular solar collectors and thermoelectric modules. *Appl. Energy* **2013**, *109*, 51–59. [CrossRef]
148. Aranguren, P.; Astrain, D.; Rodríguez, A.; Martinez, A. Experimental investigation of the applicability of a thermoelectric generator to recover waste heat from a combustion chamber. *Appl. Energy* **2015**, *152*, 121–130. [CrossRef]
149. Vian, J.; Astrain, D. Development of a heat exchanger for the cold side of a thermoelectric module. *Appl. Therm. Eng.* **2008**, *28*, 1514–1521. [CrossRef]

150. Araiz, M.; Martinez, A.; Astrain, D.; Aranguren, P. Experimental and computational study on thermoelectric generators using thermosyphons with phase change as heat exchangers. *Energy Convers. Manag.* **2017**, *137*, 155–164. [CrossRef]
151. Riffat, S.; Ma, X. Improving the coefficient of performance of thermoelectric cooling systems: A review. *Int. J. Energy Res.* **2004**, *28*, 753–768. [CrossRef]
152. Lu, X.; Zhao, D.; Ma, T.; Wang, Q.; Fan, J.; Yang, R. Thermal resistance matching for thermoelectric cooling systems. *Energy Convers. Manag.* **2018**, *169*, 186–193. [CrossRef]
153. Sakamoto, T.; Iida, T.; Sekiguchi, T.; Taguchi, Y.; Hirayama, N.; Nishio, K.; Takanashi, Y. Selection and Evaluation of Thermal Interface Materials for Reduction of the Thermal Contact Resistance of Thermoelectric Generators. *J. Electron. Mater.* **2014**, *43*, 3792–3800. [CrossRef]
154. Wang, S.; Xie, T.; Xie, H. Experimental study of the effects of the thermal contact resistance on the performance of thermoelectric generator. *Appl. Therm. Eng.* **2018**, *130*, 847–853. [CrossRef]
155. Siouane, S.; Poure, P.; Jovanović, S. Fully Electrical Modeling of Thermoelectric Generators with Contact Thermal Resistance Under Different Operating Conditions. *J. Electron. Mater.* **2016**, *46*, 40–50. [CrossRef]
156. Bjørk, R. An Analytical Model for the Influence of Contact Resistance on Thermoelectric Efficiency. *J. Electron. Mater.* **2015**, *45*, 1301–1308. [CrossRef]
157. Luo, Y.; Kim, C.N. Effects of the cross-sectional area ratios and contact resistance on the performance of a cascaded thermoelectric generator. *Int. J. Energy Res.* **2019**, *43*, 2172–2187. [CrossRef]
158. Zhang, J.; Xuan, Y. Investigation on the effect of thermal resistances on a highly concentrated photovoltaic-thermoelectric hybrid system. *Energy Convers. Manag.* **2016**, *129*, 1–10. [CrossRef]
159. Grujicic, M.; Zhao, C.; Dusel, E. The effect of thermal contact resistance on heat management in the electronic packaging. *Appl. Surf. Sci.* **2005**, *246*, 290–302. [CrossRef]
160. Lin, C.; Chung, D. Nanoclay Paste as a Thermal Interface Material for Smooth Surfaces. *J. Electron. Mater.* **2008**, *37*, 1698–1709. [CrossRef]
161. Beltrán-Pitarch, B.; Vidan, F.; García-Cañadas, J. Characterization of thermal contacts between heat exchangers and a thermoelectric module by impedance spectroscopy. *Appl. Therm. Eng.* **2020**, *165*, 114361. [CrossRef]
162. Zhang, X.; Sun, S.; Wu, Q.; Wan, N.; Pan, D.; Bai, Y. Improved electrochemical and thermal performances of layered Li[Li0.2Ni0.17Co0.07Mn0.56]O_2 via Li2ZrO3 surface modification. *J. Power Sources* **2015**, *282*, 378–384. [CrossRef]
163. Li, G.; Wang, Z.; Wang, F.; Wang, X.; Li, S.; Xue, M. Experimental and Numerical Study on the Effect of Interfacial Heat Transfer on Performance of Thermoelectric Generators. *Energies* **2019**, *12*, 3797. [CrossRef]
164. Chung, D. A review of exfoliated graphite. *J. Mater. Sci.* **2015**, *51*, 554–568. [CrossRef]
165. Díez, G.G.; Gordillo, J.M.S.; Pujadó, M.P.; Salleras, M.; Fonseca, L.; Morata, Á.; Rubio, A.T. Enhanced thermoelectric figure of merit of individual Si nanowires with ultralow contact resistances. *Nano Energy* **2020**, *67*, 104191. [CrossRef]
166. Jeong, S.; Cruz, F.J.; Chen, S.; Gravier, L.; Liu, J.; Wu, Z.; Hjort, K.; Zhang, S.-L.; Zhang, Z. Stretchable Thermoelectric Generators Metallized with Liquid Alloy. *ACS Appl. Mater. Interfaces* **2017**, *9*, 15791–15797. [CrossRef]
167. Lu, Z.; Zhang, H.; Mao, C.; Li, C.M. Silk fabric-based wearable thermoelectric generator for energy harvesting from the human body. *Appl. Energy* **2016**, *164*, 57–63. [CrossRef]
168. Lee, W.; Lee, J. Development of a compact thermoelectric generator consisting of printed circuit heat exchangers. *Energy Convers. Manag.* **2018**, *171*, 1302–1310. [CrossRef]
169. Madan, D.; Wang, Z.; Wright, P.K.; Evans, J.W. Printed flexible thermoelectric generators for use on low levels of waste heat. *Appl. Energy* **2015**, *156*, 587–592. [CrossRef]
170. Karwa, N.; Stanley, C.; Intwala, H.; Rosengarten, G. Development of a low thermal resistance water jet cooled heat sink for thermoelectric refrigerators. *Appl. Therm. Eng.* **2017**, *111*, 1596–1602. [CrossRef]



© 2020 by the authors. Licensee MDPI, Basel, Switzerland. This article is an open access article distributed under the terms and conditions of the Creative Commons Attribution (CC BY) license (http://creativecommons.org/licenses/by/4.0/).